ARL-SR-0430 • SEP 2020

4th Annual Postdoc and Early Career Research Day: CCDC Army Research Laboratory Poster Symposia and Activities

by Mary Beth Galanko, Sampath Gunukula, James Hare, Haval Kareem, Robin Kharu, Antonio Llopis-Jepsen, Lin Ma, Luther Mahoney, Sina Najmaei, Thomas Rohrabaugh, Victor Tseng, Owen Vail, Adam Wilson, Alexander Winton, Jonathan Bennion, Matthew Dunstan, Daniel Field, Andrew Rosenberger, Anthony Baker, Kanika Bansal, Chloe Callahan-Flintoft, Russell Cohen Hoffing, Shannon Moore, Christopher Sinks, Amrit Bedi, John Hyatt, Piyush Sharma, and Blake Johnson

Approved for public release; distribution is unlimited.

NOTICES

Disclaimers

The findings in this report are not to be construed as an official Department of the Army position unless so designated by other authorized documents.

Citation of manufacturer's or trade names does not constitute an official endorsement or approval of the use thereof.

Destroy this report when it is no longer needed. Do not return it to the originator.

ARL-SR-0430 ● SEP 2020

4th Annual Postdoc and Early Career Research Day: CCDC Army Research Laboratory Poster Symposia and Activities

by Mary Beth Galanko, Sampath Gunukula, James Hare, Haval Kareem, Robin Kharu, Antonio Llopis-Jepsen, Lin Ma, Luther Mahoney, Sina Najmaei, Thomas Rohrabaugh, Victor Tseng, Owen Vail, Adam Wilson, Alexander Winton
Sensors and Electron Devices Directorate, CCDC Army Research Laboratory

Jonathan Bennion, Matthew Dunstan, Daniel Field, Andrew Rosenberger
Weapons and Materials Research Directorate, CCDC Army Research Laboratory

Anthony Baker, Kanika Bansal, Chloe Callahan-Flintoft, Russell Cohen Hoffing, Shannon Moore, Christopher Sinks
Human Research and Engineering Directorate, CCDC Army Research Laboratory

Amrit Bedi, John Hyatt, Piyush Sharma
Computational and Information Sciences Directorate, CCDC Army Research Laboratory

Blake Johnson
Vehicle Technology Directorate, CCDC Army Research Laboratory

Approved for public release; distribution is unlimited.

REPORT DOCUMENTATION PAGE

Form Approved
OMB No. 0704-0188

Public reporting burden for this collection of information is estimated to average 1 hour per response, including the time for reviewing instructions, searching existing data sources, gathering and maintaining the data needed, and completing and reviewing the collection information. Send comments regarding this burden estimate or any other aspect of this collection of information, including suggestions for reducing the burden, to Department of Defense, Washington Headquarters Services, Directorate for Information Operations and Reports (0704-0188), 1215 Jefferson Davis Highway, Suite 1204, Arlington, VA 22202-4302. Respondents should be aware that notwithstanding any other provision of law, no person shall be subject to any penalty for failing to comply with a collection of information if it does not display a currently valid OMB control number.

PLEASE DO NOT RETURN YOUR FORM TO THE ABOVE ADDRESS.

1. REPORT DATE *(DD-MM-YYYY)*	**2. REPORT TYPE**	**3. DATES COVERED (From - To)**
September 2020	Special Report	September 2019

4. TITLE AND SUBTITLE
4th Annual Postdoc and Early Career Research Day: CCDC Army Research Laboratory Poster Symposia and Activities

5a. CONTRACT NUMBER

5b. GRANT NUMBER

5c. PROGRAM ELEMENT NUMBER

6. AUTHOR(S)
Mary Beth Galanko, Sampath Gunukula, James Hare, Haval Kareem, Robin Kharu, Antonio Llopis-Jepsen, Lin Ma, Luther Mahoney, Sina Najmaei, Thomas Rohrabaugh, Victor Tseng, Owen Vail, Adam Wilson, Alexander Winton, Jonathan Bennion, Matthew Dunstan, Daniel Field, Andrew Rosenberger, Anthony Baker, Kanika Bansal, Chloe Callahan-Flintoft, Russell Cohen Hoffing, Shannon Moore, Christopher Sinks, Amrit Bedi, John Hyatt, Piyush Sharma, and Blake Johnson

5d. PROJECT NUMBER

5e. TASK NUMBER

5f. WORK UNIT NUMBER

7. PERFORMING ORGANIZATION NAME(S) AND ADDRESS(ES)
US Army Research Laboratory
ATTN: FCDD-RLS-RP
Adelphi Laboratory Center, MD 20783-1138

8. PERFORMING ORGANIZATION REPORT NUMBER
ARL-SR-0430

9. SPONSORING/MONITORING AGENCY NAME(S) AND ADDRESS(ES)

10. SPONSOR/MONITOR'S ACRONYM(S)

11. SPONSOR/MONITOR'S REPORT NUMBER(S)

12. DISTRIBUTION/AVAILABILITY STATEMENT
Approved for public release; distribution is unlimited.

13. SUPPLEMENTARY NOTES
primary author's email: <adam.a.wilson6.civ@mail.mil>; ORCID(s): Adam Wilson, 0000-0003-4741-6612; Chloe Callahan-Flintoft, 0000-0002-1874-2032; Mary Galanko, 0000-0002-7769-3963; James Hare, 0000-0002-3920-7442; John Hyatt, 0000-0003-1265-9788; Shannon Moore, 0000-0002-4986-1659; Thomas Rohrabaugh, 0000-0001-6652-9781.

14. ABSTRACT
The US Army Combat Capabilities Development Command (CCDC) Army Research Laboratory (ARL) Postdoc Association (PDA) organized its 4th Annual Postdoc and Early Career Research Day to showcase research outcomes, achievements, and contributions from postdocs and early career researchers across the enterprise. The event included an invited keynote speaker, a Q&A panel, and a poster session.

This special report contains a brief summary outlining the event and the current status of CCDC Army Research Laboratory's postdoctoral and early career research communities. The contributed abstracts presented at the event and a limited number of contributed posters are appended.

15. SUBJECT TERMS
ARL Postdoc and Early Career Research Day, ARL Postdoc Association, 2019 National Postdoc Week, poster symposia

16. SECURITY CLASSIFICATION OF:			**17. LIMITATION OF ABSTRACT**	**18. NUMBER OF PAGES**	**19a. NAME OF RESPONSIBLE PERSON**
a. REPORT	**b. ABSTRACT**	**c. THIS PAGE**			**19b. TELEPHONE NUMBER (Include area code)**
Unclassified	Unclassified	Unclassified	UU	44	Adam Wilson 301-394-1984

Standard Form 298 (Rev. 8/98)
Prescribed by ANSI Std. Z39.18

Contents

List of Tables iv

Acknowledgments v

1. Introduction 1

2. Engagement Across the Laboratory 2

Appendix A. Contributed Abstracts Presented at the 4th Postdoc and Early Career Research Day 4

Appendix B. Contributed Posters Presented at the 4th Postdoc and Early Career Research Day 15

List of Symbols, Abbreviations, and Acronyms 36

Distribution List 37

List of Tables

Table 1 List of postdoctoral fellows who presented at the symposia. Note: Abbreviations are listed in the acronyms list. ……3

Acknowledgments

The 4th Annual Postdoc and Early Career Research Day (4PECRD) Organizing Committee would like to thank the dedicated work and support of US Army Capabilities Development Command (CCDC) Army Research Laboratory's (ARL's) administrative staff. These include, but are not limited to, Ms Jenna C Brady, Ms Evelyn Bond, Mr William Parks, Mr Eric Proctor, and many more. The committee would also like to thank the CCDC Army Research Laboratory Fellows and science and technology leaders (Dr Richard Becker, Dr Robert Benoit, Dr Stephen Berkebile, Dr John Clayton, Dr Piotr Franaszczuk, Dr Lance Kaplan, Dr Rose Pesce-Rodriguez, Dr Brian Sadler, and Dr Jeffrey Veals) who volunteered their time to judge the poster session. Lastly, we want to thank the panelists (Dr Michael Wraback, Dr Daniel Miracle, Dr Kyle Grew and Sgt Maj Snipes) for a great Q&A session.

Finally, we must recognize the 4PECRD Organizing Committee, which was formed by a group of dedicated volunteer postdocs. Their hard work enabled the success of the 4PECRD.

- Matthew Dunstan (Weapons and Materials Directorate)
- Adam Wilson (Sensors and Electron Devices Directorate)
- Owen Vail (Sensors and Electron Devices Directorate)
- Mary Beth Galanko (Sensors and Electron Devices Directorate)
- Shannon Moore (Human Research and Engineering Directorate)
- Piyush Sharma (Computational and Information Sciences Directorate)

This research was supported in part by an appointment to the Postgraduate Research Participation Program at ARL administered by the Oak Ridge Associated Universities through an interagency agreement between the US Department of Energy and ARL.

1. Introduction

The 4th Annual Postdoc and Early Career Research Day (4PECRD) is a US Army Combat Capabilities Development Command (CCDC) Army Research Laboratory (ARL) Postdoc Association (PDA) initiative to commemorate postdoctoral and early career executed and led research across CCDC Army Research Laboratory. It was planned to coincide with the 2019 National Postdoc Week in celebration of ARL's postdoctoral cohort. The goal is to bring awareness to the important research being performed by postdocs and early career researchers across the organization and further promote collaboration where suited. Mainly, the 4PECRD is a venue to celebrate and promote the postdoctoral and early career experience at ARL.

This was the fourth iteration of this event and was held on 19 September 2019 at ARL's Laboratory Center in Adelphi, Maryland. The 4PECRD included a panel session where postdoctoral fellows were able to interact with current ARL civilians with a diverse perspective of what enables success at ARL. Each of the panelists represented a different stage and trajectory of career, and brought a unique and rich perspective to the discussion. A total of 29 postdocs presented posters, and many others attended other activities such as the Q&A panel.

The 4PECRD objectives were as follows:

- Recognize contributions from postdocs and early career researchers to current state-of-the-art research and discovery at ARL.
- Foster collaborative research among postdocs with common research interests.
- Serve as an interactive platform for postdocs and upper management.
- Provide insights into how to develop a success career as an Army scientist.

This Special Report provides a snapshot of the 4PECRD. An abstract book and limited number of contributed posters are published as Appendixes.

2. Engagement Across the Laboratory

A total of 29 postdocs and early career researchers presented posters, and these are listed in Table 1 with their location and directorate affiliation. The distribution across directorates shows a significant decrease in participation by the Weapons and Materials Research Directorate (WMRD), which is traceable to a strong reduction the number of postdocs in that directorate. Due to a reduction in postdoc numbers across the lab, this was the first year that the symposium was opened to include participation from early career researchers throughout the lab. Despite the reduction in the number of postdoctoral fellows at ARL, the number of abstracts submitted for this year's event surpassed that of 2017 (29 vs. 26), indicating good engagement with the postdoc and early career workfoce, and support from mentors and management of the postdoctoral cohorts. The abstract book created to advertise the event has been appended at the end of the report, Appendix A. A limited number of contributed posters can be found in Appendix B.

Table 1 List of postdoctoral fellows who presented at the symposia. Note: Abbreviations are listed in the acronyms list.

Presenter	Directorate	Location
Baker, Anthony	HRED	Aberdeen Proving Ground (APG)
Bansal, Kanika	HRED	APG
Bedi, Amrit	CISD	Adelphi Laboratory Center (ALC)
Bennion, Jonathan	WMRD	APG
Callahan-Flintoft, Chloe	HRED	APG
Cohen Hoffing, Russell	HRED	ARL-West
Dunstan, Matthew	WMRD	APG
Field, Daniel	WMRD	APG
Forster, Daniel	WMRD	APG
Galanko, Mary Beth	SEDD	ALC
Gunukula, Sampath	SEDD	ALC
Hare, Zach	SEDD	ALC
Kareem, Haval	SEDD	ALC
Hyatt, John	CISD	ALC
Johnson, Blake	VTD	ARL-Central
Kharu, Robin	SEDD	ALC
Llopis, Antonio	SEDD	ALC
Ma, Lin	SEDD	ALC
Mahoney, Luther	SEDD	ALC
Moore, Shannon	HRED	APG
Najmaei, Sina	SEDD	ALC
Rohrabaugh, TJ	SEDD	ALC
Rosenberger, Andrew	WMRD	APG
Sharma, Piyush	CISD	ALC
Sinks, Christopher	HRED	APG
Tseng, Victor	SEDD	ALC
Vail, Owen	SEDD	ALC
Wilson, Adam	SEDD	ALC
Winton, Alexander	SEDD	ALC

Appendix A. Contributed Abstracts Presented at the 4th Postdoc and Early Career Research Day

The Postdoctoral Association's 4th Annual ARL Postdoc and Eary Career Research Day

ABSTRACT BOOK

18 Sep 2019
Adelphi, MD

This page is intentionally left blank
Document typeset with LaTeX

REFLECT: A Methodology for Capturing Team Communication Flow in Real-Time

Baker, Anthony L.[1], *Brewer II, R.W.*[2], *Schaefer, K.E.*[3] *and Hill, S.G.*[1]

[1]CCDC Army Research Laboratory, **FCDD-RLH-FD**, APG, MD, [2]CCDC Army Research Laboratory, **FCDD-RLV-A**, APG, MD, [3]CCDC Army Research Laboratory, **FCDD-RLH**, APG, MD

*corresp. author: anthony.baker42.ctr@mail.mil

This poster details development and initial usability of the Realtime Flow, Event, and Coordination Tool (REFLECT). This tool allows a user to pature team communication flow in realtime. This is critical for advancing Army initiatives in human-autonomy teaming (HAT) as outlined by CCDC Army Research Laboratory's HAT Essential Research Program (ERP) because communication flow affects, and is affected by, intelligent systems interactions, team structures, and tasking demands. As such, communication flow data can be used to understand and evaluate peformance, and, in human-autonomy teams, such data provides a novel metric of team trust and cohesion. In our initial usability assessment, participants used REFLECT to capture team communication flow using autio recordings from the US Army Wingman JCTD where a 5-man crew of Marines engaged in mounted machine gun live fire exercises involving a manned-unmanned team. After using REFLECT, participants completed surveys and interviews to gather feedback on the design of the tool and on the task of capturing communication data. The initial look at the usability feedback suggests that the tool is easy to use, but ares for improvement exist specific to data visualization features, better integration with event loggers/data sources, and integration with artificial intelligence and machine learning. The next tool version will be tested during upcoming US Army Wingman lethality events, field exercises, and INFORMS Lab simulation studies, supporting advanced research for developing appropriate communication metrics of team trust and team cohesion across future ARmy human-autonomy teams. All project efforts support Army Modernization Priorities and NGCV goals.

Partial synchrony and chimera states in human brain networks

Bansal, Kanika[1,2], *Garcia, J.O.*[1,3] *and Vettel, J.M.*[1,3,4]

[1]CCDC Army Research Laboratory, **FCDD-RLH-FB**, APG, MD, [2]Department of Biomedical Engineering, Columbia University, New York, NY, [3]Department of Bioengineering, University of Pennsylvania, Philadelphia, PA, [4]Department of Psychological and Brain Sciences, University of California, Santa Barbara, CA

*corresp. author: phy.kanika@gmail.com

Partial synchronization is ubiquitous to the dynamics of complex real-world systems. The human brain, a complex biological system, functions through the emergence of coherent and incoherent activity between distributed neuronal components. This activity balances the segregation of information for localized processing while also maintaining efficient integration of information for global coordination. Human cognition relies on the states of partial synchrony, including chimera states with separate domains of synchronized and de-synchronized dynamics. We propose that spatial patterning of these partial synchrony states plays a fundamental role in individual variability in cognitive performance. In our recent paper (Bansal et al. 2019, Sci Adv), we used a chimera-based framework to capture individual differences in structurally-constrained computational models of the brain. Our ongoing research extends this work from individual brains to team performance. Our research posits that patterns of coherent and incoherent activity emerge in teams, and we hypothesize that team outcomes can be predicted by discovering the spatial patterning of partial synchrony states. For example, teams interact by sharing ideas, and the temporal evolution of how subgroups form cohesive or conflicting opinions likely captures how a joint decision is eventually determined. By understanding general principles behind these patterns, our work can identify opportunities to enhance team performance by facilitating dynamic team composition. This approach can be applied for human-human, human-agent, and agent-agent teams, and thus, our work unravels dynamic features that are critical for the envisioned future Army battlefield with hundreds, if not thousands, of interconnected human and autonomous agents. ***Best Poster Award***

Online Learning with Kernels Against Dynamic Comparators

Bedi, Amrit Singh[1], *Koppel, A.*[1], *Rajawat, K.*[2]

[1]CCDC Army Research Laboratory, **RDRL-SEE-E**, Adelphi, MD, [2]Department of Electrical Engineering India Institute of Technology Kanpur, Kanpur, India

*corresp. author: amritbd@iitk.ac.in

An open challenge in supervised learning is conceptual drift: a data point begins as classified according to one label, but over time the notion of that label changes. Beyond linear autoregressive models, transfer and meta learning address drift, but require data that is representative of disparate domains at the outset of training. To relax this requirement, we propose a memory-efficient online universal function approximator based on compressed kernel methods. Our approach hinges upon viewing non-stationary learning as online convex optimization with dynamic comparators, for which performance is quantified by dynamic regret. Prior works control dynamic regret growth only for linear models. In contrast, we hypothesize actions belong to reproducing kernel Hilbert spaces (RKHS). We propose a functional variant of online gradient descent (OGD) operating in tandem with greedy subspace projections. Projections are necessary to surmount the fact that RKHS functions have complexity proportional to time. For this scheme, we establish sublinear dynamic regret growth in terms of both loss variation and functional path length, and that the memory of the function sequence remains moderate. Experiments demonstrate the usefulness of the proposed technique for online nonlinear regression and classification problems with nonstationary data, addressing drift.

High-Pressure Characterization of High-Performance Insensitive Energetic Materials: Dihydroxylammonium 5,5'-Bis(3-Nitro-1,2,4-Triazolate-1N-Oxide) (MAD-X1)

Bennion, J.C.[1], *Ciezak-Jenkins, J.A.*[1], *Jenkins, T.A.*[1]

[1]CCDC Army Research Laboratory, **FCDD-RLW-LB**, APG, MD

*corresp. author: jonathan.c.bennion.civ@mail.mil

The high-pressure behavior of dihydroxylammonium 5,5'-bis(3-nitro-1,2,4-triazolate-*1N*-oxide) (MAD-X1) was studied at room temperature to 25 GPa by Raman spectroscopy and powder X-ray diffraction. No evidence of polymorphism was observed over this pressure range, indicating that the ambient structure of MAD-X1 remains stable up to conditions similar to the detonation pressure of the material. Additionally, such findings suggest that this high performance material can serve as an insensitive RDX replacement in energetic formulations without the concern of uncontrolled polymorphism that might otherwise affect the performance and safety of the munition. These results are important for understanding the behavior of bis-1,2,4-triazoles and N-oxide derivatives at high-pressure. General trends involving hydrogen bonding are seen to correspond to large regions of structural stability over the relevant range for most energetic applications. This further suggests the importance of these network structures in designing insensitive systems.

The attentional drag: how feature temporal autocorrelation and visual transients extend and close attentional windows in time

Callahan-Flintoft[1]

[1]CCDC Army Research Laboratory, **FCDD-RLH-FC**, APG, MD

*corresp. author: chloe.a.callahan-flintoft.civ@mail.mil

Exploring how the attentional system samples from continuously changing input is important for understanding and optimizing how soldiers perform common visual search tasks in natural environments. To study how the brain selects information in time, researchers sequentially presented discrete stimuli (e.g. letters) to participants and found that attention deploys rapidly in response to a cue with an average selection latency of under 25 ms (Goodbourn & Holcombe, 2015). However in paradigms where features changed smoothly (as is typical in the real world), the selection latency can be as large as 400 ms (Sheth, Nijhawan, & Shimojo, 2000). Three experiments explored this discrepancy by having participants monitor two changing color disks (changing smoothly or pseudo-randomly). During each trial, a cue (white ring) flashed around one of the disks. Participants used a continuous scale to report the disk's perceived color at the time of the cue. Experiment 1 found selection was delayed by over 100 ms with smoothly compared to randomly changing color. Experiment 2 found this delay was further increased (32 ms) when smoothness increased. Finally, Experiment 3 found that this delay occurs when smooth change is presented after the cue rather than before. To account for these results, the "attentional drag" theory, implemented as a computational model, proposes that when attention is deployed in response to a cue, smoothly changing features temporally extend attentional engagement whereas a sudden feature change causes rapid disengagement. The prolonged duration of attentional engagement in the smooth condition yields longer latencies in selecting feature information.

Task-independent pupil features uniquely predict vigilance performance

Cohen Hoffing, R.[1], *Thurman, S.*[1], *Garcia, J.*[1] *and Vettel, J.*[1]

[1]CCDC Army Research Laboratory, **FCDD-RLH-FB**, ARL-WEST

*corresp. author: russell.a.cohenhoffing.civ@mail.mil

The pupil response allows for a non-invasive measure of cognitive processes, but pupil size is also strongly driven by non-cognitive factors that confound the task-dependent pupil response. This limitation can hinder generalizability of psychologically meaningful pupil features to other contexts. To overcome this obstacle, we leverage a unique longitudinal pupillometry data set to identify task-independent pupillary features. In this data set, participants (n=31) completed a battery of cognitive tasks on 8 biweekly sessions over the course of 16 weeks This design allowed us to address two critical questions about identifying task-independent pupil features: (i) which pupil features are reliably related across tasks, and (ii) do these pupil features reflect the influence of cognitive processes on behavior? Results indicate two features that are highly consistent across tasks –baseline pupil diameter and pupil motility, a novel metric that captures the distribution of pupillary movements over time. To investigate our second question, we analyzed the relationship between pupil features and performance in each task. Results indicate that larger baseline and lower motility were uniquely associated with faster response times in the psychomotor vigilance task, even when these metrics were derived from other tasks. Research suggests that pupil motility and baseline, respectively, reflect parasympathetic and sympathetic contributions to behavior. These findings support ongoing research to identify robust, generalizable physiological signals that can be used to infer human states. Pupillometry is a low-cost, portable, and minimally-invasive modality that could improve autonomous agents' understanding of human states to optimize human performance.

The use of hydrogen in titanium additive manufacturing

Dunstan, M.[1]*,Butler, B.*[1] *and Paramore, J.*[1]

[1]CCDC Army Research Laboratory, **FCDD-RLW-MF**, APG, MD

*corresp. author: matthew.k.dunstan.civ@mail.mil

In recent years, additive manufacturing (AM) has shown to be a promising method for reducing the cost and increasing the complexity of titanium components with the majority of research focusing on melt-based methods (i.e. powder bed fusion and directed energy deposition). However, as these methods rely on melting the feed material, which results in highly isotropic microstructures that can be detrimental to mechanical properties. In an effort to mitigate these challenges, the use of hydrogen as a temporary alloying element has been identified as a promising method to prevent and/or reset unfavorable microstructures in AM Ti-6Al-4V. Specifically, the hydrogen sintering is used in conjunction with a solid-state AM method known as fused filament fabrication (FFF). Additionally, a new post-AM heat treatment called Thermal Hydrogen Refinement of Microstructure (THRM) is used to reset the microstructure in several melt based AM processes.

High Strain Rate Behavior of Medium−Mn TRIP Steel

Field, D.M.[1]*,Buchley, M.F.*[2]*, and Van Aken, D.C.*[2]

[1]CCDC Army Research Laboratory, **FCDD-RLW-MF**, APG, MD, [2]Missouri University of Science and Technology, Rolla, MO

*corresp. author: daniel.field8.civ@mail.mil

Two Medium-Mn TRIP steels were produced with varying levels of aluminum to create steels with two different starting microstructures; γ-austenite and α-martensite and an ϵ-martensite and α-martensitic structure. Dynamic compression and tension testing using a Split-Hopkinson Pressure Bar (SHPB) was performed to characterize each steel under different loading conditions. A flow stress asymmetry was noted for the two alloys depending on the starting microstructure. It was found that alloys containing γ-austenite in the starting structure had a higher flow stress in tension than the alloy containing ϵ-martensite. The opposite was observed in compression. This material response is rationalized based upon volume transformation during the deformation induced martensitic reactions: $\gamma \rightarrow \epsilon$ (ΔV<0) or $\epsilon \rightarrow \alpha$ (V > 0). Both alloys however, exhibited a positive strain rate response with flow stress; the γ-austenite containing steel exhibited a positive strain rate response with the reduction in area as measured on the fractured tensile bars. ***Best Poster Award***

AT-cut Quartz Piezoelectric Transformers for Passive Voltage Gain in an RF Front-end

Galanko, M.B. [1]*, Bedair, S.S.* [1]*, Rudy, R.* [2]*, Tseng, V.* [1]*, Pulskamp, J.* [2] *and Kierzewski, I.*[1]*,*

[1]CCDC Army Research Laboratory, **FCDD-RLS-DE**, Adelphi, MD, [2]CCDC Army Research Laboratory, **FCDD-RLS-RL**, Adelphi, MD

*corresp. author: mary.e.galanko.civ@mail.mil

The purpose of this work is to assess the performance of an AT-cut quartz device as a two−port resonant transformer for near−zero power−consuming wake−up receiver applications. Wake−up receivers enable distributed, persistent low−power communications within the "Internet of Things." These capabilities are important for the Army to remotely monitor contested environments. A wake−up receiver must be highly sensitive to low−power radio signals yet consume minimal power (< 100 nW) until a signal of interest is present. The quartz resonant transformer in this work serves as a front-end for the receiver and helps fulfill system requirements by providing high passive voltage gain, impedance matching, and high-Q filtering around its resonant frequency. The device consists of two coupled thickness-shear mode trapped-energy ∼50 MHz resonators on a single quartz substrate. Passive voltage gain up to 84 V/V (referenced to 50 Ω) is observed when the device is driven by a low-power signal (≤ -30 dBm) at resonance. For various load impedances, its voltage gain approaches or exceeds that of other front-ends currently used in wake-up receivers. Additionally, this work shows that connecting two coupled-resonator quartz devices in a parallel-input, series-output (PISOT) configuration can further improve voltage gain. A 17% increase in gain is demonstrated for PISOT over that of a single coupled resonant transformer for various load impedances. This work is the first use of quartz piezoelectric transformers (PTs) for passive voltage gain, and the highest open-circuit gain demonstrated in a two-port micromechanical PT.

Advanced Catalysts and Pyrolysis Process for Upgrading Biomass to Useful Chemicals/Fuels

Gunukula, S.[1]*, Emdadi, L.*[1] *and Tran, D.*[1]

[1]CCDC Army Research Laboratory, **FCDD-RLS-DE**, Adelphi, MD

*corresp. author: sampath.gunukula@gmail.com

This research aims the development of a compact pyrolysis process to upgrade locally available, low energy density biomass i.e., convert grass or wood-based materials to valuable, high energy density chemicals/fuels that are stable for extended periods. This project has two primary focus areas: (1) synthesizing novel catalytic materials and (2) investigating new pyrolysis reactor designs for the efficient conversion of biomass and oxygenated intermediates (acids/alcohols) to hydrocarbon fuels (gasoline or jet fuel). To guide the design of a new pyrolysis reactor, simulation and modeling studies are helping to determine the size, weight, and efficiency of converting biomass to value-added chemicals/fuels. These efforts will have significant impact for augmenting the Army's robotic autonomous systems by increasing mission length on-demand and reducing the energy logistics burden.

Non-Bayesian Social Learning with Uncertain Models

Hare, J.Z.[1] *and Kaplan, L.*[1]

[1]CCDC Army Research Laboratory, **FCDD-RLS-SA**, Adelphi, MD

*corresp. author: james.z.hare.civ@mail.mil

Non-Bayesian social learning (NBSL) theory provides an attractive framework that allows for distributed inferencing of a group of agents communicating over a social network through repeated interactions. In this framework, each agent sequentially forms and updates their opinions on the true state of the world using a social learning rule and the likelihood of a new observation conditioned on a predefined model. Traditionally, this likelihood is assumed to be dogmatic, i.e., the parameters are known precisely, due to the availability of a significantly large set of labeled training data to learn them. However, in many realistic scenarios, the agent may have limited access to training data, due to data collection costs or measurement imprecisions, resulting in a likelihood model that is uncertain. In this regard, we propose to model the likelihood parameters as a second-order distribution, which allows knowledge of the likelihood to be conditioned on the prior evidence (training data) rather than treated as precise point values. Then, we incorporate this uncertainty into NBSL theory and study the implications of such uncertain models. We formulate a new hypothesis testing approach that studies the consistency of the prior evidence with the new observation sequence, which evaluates each hypothesis on their own merit to ensure unbiased conclusions due to the amount of prior evidence. Interestingly, as the amount of prior evidence tends to infinity, absolute learning occurs and is the same as traditional NBSL theory. Thus, incorporating uncertain models into NBSL theory generalizes the problem for any amount of prior evidence.

Beyond validation accuracy: How to develop a machine learning model you can trust and understand

Hyatt, J.[1] *and Lee, M.*[1]

[1]CCDC Army Research Laboratory, **FCDD-RLC-NB**, Adelphi, MD

*corresp. author: john.shelton.hyatt11.ctr@mail.mil

Machine learning (ML) will play an increasingly important role in the Army's future data analysis and decision making processes. However, in both industry and academia across the entire field, ML classifier development exclusively optimizes the model to maximize validation accuracy, a necessary metric that is nevertheless insufficient to assess whether a model will likely perform well in the real world. Specifically, a model with high validation accuracy may be vulnerable to adversarial attacks or misclassify (with high confidence) real-world data different than the data in its training set. It may also be incomprehensible to a human or base its decisions on a small subset of available features, ignoring others of equal importance. While these problems have been the focus of a substantial amount of recent research, and despite recurring news coverage, they are not considered during model development, and at best are addressed after the fact – sometimes after a flawed model has done a substantial amount of damage in the real world. We believe that, in addition to validation accuracy, the model development process must give equal weight to other performance metrics such as explainability, resistance to adversarial attacks, and overconfident predictions on out-of-distribution data. Using free, readily-available tools, we incorporate these assessments into the model design process to differentiate between convolutional neural network classifiers trained on the notMNIST character dataset. Specifically, we show that ensemble and ensemble-like models with high cardinality outperform simple models with identical validation accuracy by up to a factor of 5 on these other metrics.

Tribological modeling of US Army fuel injection pumps running with non-optimal fuels

Johnson, B..[1]*, Berkebile, S.*[1]*, Murthy, N.*[1] *and Pickens, D.*[1]

[1]CCDC Army Research Laboratory, **FCDD-RLV-P**, ARL-C, IL,

*corresp. author: blake.a.johnson77.civ@mail.mil

A broadening of the acceptable range of fuels used in Army combustion engines would greatly enhance the durability, adaptability, and expeditionary abilities of Army vehicles. A key component in this improvement is the development of fuel injection systems that can function using a wider range of viscosities and chemical compositions. Non-optimal fuel usage presents numerous challenges from wear and deterioration of fuel injection systems. A commonly used diesel fuel injection pump (Bosch CP3) has been studied in order to determine how its design and materials are connected to performance and commonly observed failure modes. A computational tribological model was developed to predict interfacial conditions based on fuel fluid properties, materials selection and operational conditions. The model considers thermal and elastic deformation, pressure and temperature-dependent fluid properties, and solid asperity contact forces, and outputs the fluid film thickness and pressure profiles, as well as friction forces throughout the pumping cycle.

Catalytic Oxidation of Propane over Palladium Alloyed with Gold: An Assessment of the Chemical and Intermediate Species

Kareem, H.[1] *and Tran, D.*[1]

[1]CCDC Army Research Laboratory, **FCDD-RLS-DE**, Adelphi, MD

*corresp. author: haval.r.kareem.civ@mail.mil

Volatile organic compounds (VOCs) including propane, carbon monoxide, nitrogen oxides are main constituents of exhaust gas emission from military bases and transportation vehicles, such as tanks, infantry fighting vehicles, armored personnel carriers etc. With growing environmental and health, an active and stable catalysts will play a vital role in the full removal of harmful gases. Catalytic combustion is considered a more efficient way for CO, and propane removal compared to thermal decomposition, which requires higher pressure and temperature. Understanding the catalytic oxidation of propane is important for developing catalysts not only for catalytic oxidation of hydrocarbons in emission systems but also for selective oxidation in chemical processing industry. For palladium-based catalysts, little is known about the identification of the chemical or intermediate species involved in propane oxidation. In this work, we describe findings of an investigation of the catalytic oxidation of propane over Al_2O_3 and TiO_2-supported palladium nanoalloys with different compositions of gold (Pd_nAu_{100-n}), focusing on probing

the chemical and intermediate species on the catalysts in correlation with the bimetallic composition and the alloying phase structure. In addition to an enhanced catalytic activity, a strong dependence of the catalytic activity on the bimetallic composition was revealed, displaying an activity maximum at Pd:Au ratio of 50:50 in terms of reaction temperature. Importantly, subtle differences of chemical and intermediate species have been identified for the catalysts with different composition of gold by in-situ measurements using Diffuse Reflectance Infrared Fourier Transform Spectroscopy (DRIFTS).

CVD growth and properties of on-axis vanadium doped semi-insulating 4H-SiC epilayers

Karhu, R.[1], *Sveinbjöornsson, E.*[2,3], *Magnusson, B.*[4], *Ivanov, I.*[2], *Danielsson, Ö.*[2] *and Ul Hassan, J.*[2]

[1]CCDC Army Research Laboratory, **FCDD-RLS-EM**, Adelphi, MD, [2]Department of Physics, Chemistry and Biology (IFM), Linköping University, [3]Science Institute, University of Iceland, [4]Norstel AB

*corresp. author: robin.karhu@gmail.com

Semi-insulating (SI) 4H-SiC is important for the growth of high-frequency devices, such as SiC-based high-power microwave devices and GaN-based high electron mobility transistor (HEMT) devices, where SI 4H-SiC is used as a substrate. These devices require SI substrates in order to reduce losses due to parasitic capacitances. The SI properties of 4H-SiC can be realized by introducing defects, these defects act as recombination centers and can compensate shallow dopants. In this study these defects have been vanadium that has been introduced during homoepitaxy in the form of vanadium tetrachloride (VTC; VCl_4). Additionally, in order to use the 4H-SiC as a substrate for GaN-based devices the 4H-SiC needs to be on-axis, this means that the surface normal is parallel with the c-axis. In this study SI homoepitaxial 4H-SiC layers has been grown using chemical vapor deposition (CVD). The CVD growth has taken place on on-axis 4H-SiC substrates. Homoepitaxial growth on on-axis substrates due to the polymorphic nature of SiC, where the different polytype exists as different stacking sequences of the Si-C bilayers. This makes it hard to achieve homoepitaxial layers without foreign polytype inclusions. The morphology of the epitaxial layers has been studied with optical microscopy. The SI properties have been verified by current-voltage measurements and low temperature photoluminescence (LTPL) measurements.

Photon Detection Confidence: A Methodology for Comparing Single Photon Detection Performance across Devices and Applications

Llopis, A.[1], *Haughn, C.*[1], *Kelly, S.*[1], *Olver, K.*[1], *Wraback, M.*[1] *and Sampath, A.*[1]

[1]CCDC Army Research Laboratory, **FCDD-RLS-EI**, Adelphi, MD

*corresp. author: antonio.llopis-jepsen.ctr@mail.mil

Single photon detectors such as single photon avalanche detectors (SPAD) and photo-multiplier tubes (PMTs) are an essential component for various applications of interest within CCDC ARL including Light Detection and Ranging (LIDAR), UV Communications and Bio-sensing/chemical detection. Device performance for single-photon detection devices, SPAD or otherwise are most often reported with two numbers: the single photon detection efficiency (SPDE)—also referred to as the photon detection efficiency or single photon quantum efficiency—and the dark count rate (DCR). The former represents the probability that a photon incident on the detector produces a count, and the latter represents the rate at which spurious counts occur (e.g. those caused by thermally generated carriers causing an avalanche within a SPAD). These figures of merit (FOMs), while the widely used, are ill-suited for directly comparing the performance of different devices for a given application, and provide no means of determining the ideal operating point for devices such as SPADs where their DCR and SPDE vary widely across their operating voltage range. In this work we discuss calculation of the photon detection confidence (PDC) for a device in a given application. The PCC takes into account both DCR, SPDE, as well as the application's anticipated photon flux, giving a probability-based FOM to pair with SPDE. We show how SPDE and PDC can guide both device selection and ideal operating parameters for a given device based our chosen application.

Highly Reversible and Rechargeable Safe Zn Batteries Based on Concentrated Aqueous Electrolyte Systems

Ma, L.[1], *Ding, M.*[1], *Borodin, O.*[1], *Ho, J.*[1] *and Xu, K.*[1]

[1]CCDC Army Research Laboratory, **FCDD-RLS-DC**, Adelphi, MD

*corresp. author: liam.l.ma.civ@outlook.com

Zn metal is an attractive anode electrode material for next generation batteries. However, dendrite growth and unsuitable pairing with cathode electrode limited the way towards widespread commercialization of Zn batteries. In this work, Zn(TFSI)2 containing concentrated aqueous electrolytes were used to obtain a highly stable and dendrite-free Zn anode, which showed stable stripping/plating for over 1000 hours. The electrolytes displayed excellent compatibility with both Zn anode and Na2V6O16·1.63H2O (HNVO) cathode for a Zn cell. The full cell demonstrated a long cycling stability at both 30oC and -20oC. Improving the U.S. Army's capacity to effectively store energy is of paramount importance—both to achieving its recently developed modernization priorities and to ensuring future technical overmatch. This work directly addresses the objective by developing novel alternative energy storage solutions with high energy density and long lifetime. It is expected this novel Zn batteries could be used for next generation combat vehicles (NGCVs) and future vertical lift systems, which demand disruptive new energy storage platforms to ensure future technical dominance.

Factors Effecting Metal Doping on Two-Dimensional and Three Dimensional Mordenite Framework Inverted (MFI) Zeolite for Chemical Energy Dense Production

Mahoney, L.[1]*, Emdadi, L.*[1] *and Tran, D.*[1]

[1]CCDC Army Research Laboratory, **FCDD-RLS-DE**, Adelphi, MD

*corresp. author: luther.j.mahoney.ctr@mail.mil

Our motivation included developing dense chemical energy that could be used on demand for extended periods of time. The U. S. Army has the seven day mission challenge and beyond. This research endeavor addresses the needed portable energy demand applications for use in long-time periods by producing higher chemical storage energy media. The chemical process involved taking ethylene gas, which can come from dehydration of bio-ethanol, and converting using MFI meso/microporous zeolite catalysts to produce alkylated aromatics. The ethylene subjected under optimal conditions with 8 h reaction period; 0.41 h-1 (WHSV); 400 °C reaction temperature; and atmospheric pressure produced up to 70% liquid products of energy dense aromatic compounds range of kerosene, according to micro-gas-chromatography (micro-GC). The energy content was determined to be 40 MJ/kg similar to gasoline. The liquid product yield varied from 29.5% to 41.2% depending on the dopant and type of zeolite structure. This research work shows that careful adjustment of metal dopant type, dispersion, and pore morphology lead to the highest mono-alkylated benzene derivatives. This experimental work can be scaled in portable on-demand use in soldier and related military applications to meet the endeavor of seven day U. S. Army mission challenge.

The Effects of Partner Knowledge in Virtual Reality

Moore, S.[1] *and Guess, M.*[1]

[1]CCDC Army Research Laboratory, **FCDD-RLH-FC**, APG, MD

*corresp. author: shannon.m.moore43.civ@mail.mil

Efficient teaming is vital to the Army, yet the quality of teamwork can vary immensely. Thus, research is needed to identify factors that contribute to successful team work. One particular goal in the area of human autonomy teaming is to improve the ability to predict teammates' behavior and understand their reasoning. It has been proposed that just as our own attitudes are functional, knowledge of others' attitudes should contribute to greater understanding of and better interactions with others (e.g., Sanbonmatsu et al., 2011). We adapted a measure of attitude familiarity (e.g., knowledge of another person's attitudes), making the assessment of attitudes specific to a joint task and thus appropriate for use with professional teams. Teams of two were recruited, resulting in 24 pairs. Pairs worked together using desktop monitors and also in virtual reality to utilize sociocultural information in order to answer questions and solve problems as a team. Pairs were randomly assigned to either engage in a discussion of their task-relevant attitudes with one another (e.g., virtual reality, word problems) for 10 minutes or to a control condition. A manipulation check found that those in the Familiar condition were significantly more aware of their partners' unique attitudes compared to those in the Control condition (p ¡ .05). Results found that those teams assigned to learn each other's task-relevant attitudes saw improved performance when working with novel technology (i.e., virtual reality) compared to those pairs in the control condition.

Reconfigurable Electronic and Phononic Properties in Super-sandwich Heterostructures of Organometallic Molecules and Layered HfS_2

Najmaei, S.[1]*, Ekuma, C.*[2]*, Wilson, A.A.*[3] *and Dubey, M.*[1]

[1]CCDC Army Research Laboratory, **FCDD-RLS-EE**, Adelphi, MD, [2]Department of Physics, Lehigh University, Bethlehem, PA, [3]CCDC Army Research Laboratory, **FCDD-RLS-DP**

*corresp. author: sina.najmaei.civ@mail.mil

Reconfigurability is a highly desired material property and essential to the future developments in sensors and computing devices. 2D van der Walls layers are a unique set of materials with distinct structural traits that are being explored in advance device applications. Here we present a versatile approach to reconfigure the electron and phonon behavior in 2D hafnium disulfide, through intercalation of organometallic sandwich compounds. Our theoretical and experimental examination of physical properties of these super-sandwich structures indicate significant changes in the electronic and vibrational properties of HfS_2. We explore the underlying mechanisms involved and demonstrate major dynamic tunability in the anisotropic thermal and electrical conductivities of the hybrid materials. The cross-plane thermal and cross-plane electrical conductivities of device made on these hybrid materials exhibit a dynamic tunability ranging 4x and 1000x, respectively. Our findings reveal a comprehensive approach for dynamic control of 2D material properties and promises unique applications in high performance electronic and phononic devices.

Design, Synthesis, and Photophysical Investigation of Novel Iridium(III) Acetylacetonate Bisphenylquinoline Complexes

Rohrabaugh, T.[1]*, O'Donnell, R.*[1]*, Ensley, T.*[1]*, Ferry, M.*[1] *and Shensky, W.*[1]

[1]CCDC Army Research Laboratory, **FCDD-RLS-EL**, Adelphi, MD

*corresp. author: thomas.n.rohrabaugh.civ@mail.mil

Due to their tunable photoreactivity and light absorbing properties, organometallic iridium(III) complexes have a wide variety of applications such as phosphorescent dopants in organic light emitting diodes (OLEDs), chemical sensing, light harvesting for solar cells, and photodynamic therapy. Particularly, our team is interested in their non-linear optical (NLO) properties such as reverse saturable absorption (RSA) and two-photon absorption (2PA). A series of iridium(III) complexes of structure $[Ir^{III}(C\wedge N)_2(acac)]^0$ (where acac = acetylacetonate and C∧N = 2-phenylquinoline and its derivatives) were synthesized to investigate the structural and electronic effects on the photophysical properties of these complexes by the addition of a nitro group and a phenyl group to the C∧N ligand, see structure below. The syntheses, chemical characterization, and photophysical properties of these iridium(III) complexes will be discussed in detail herein.

IoT in Smart Cities: Information Theoretic and Deep Learning Approaches to Improve Parking Solutions

Sharma, P.[1] *and Raglin, A.*[1]

[1]CCDC Army Research Laboratory, **FCDD-RLC-IB**, Adelphi, MD

*corresp. author: piyush.k.sharma.ctr@mail.mil

The smart city is an emerging concept which appears to be a promising approach not only in urban environment to accomodate the growing needs and to improve the quality of life, but also in military environment for installing and integrating network-connected sensors into the everyday operations. This demands the use of information technologies, digitization, and urban traffic planning for better mobility. Internet of Things (IoT) devices (wireless sensors, actuators, meters, etc.) come in handy to collect and analyze data. Because military bases share many of the same characteristics as small cities, depend on many common electronic architectures and devices used in civilian environment, and the IoT gaining more traction, this concept can be applied to military installations. The modernized smart bases improve parking, logistics, reduce costs, and help military staffers make better decisions in caily C2 (command and control) routine. Impetus behind this work stemmed from Army's existing challenge to carry out its Multi-Domain Operations (MDO) effectively. We set out to deveop a model for covercoming limitations of existing machine/deep learning methods in order to predict the parking availability in IoT environment for smart cities when faced with data nuances, noise and nonlinearity challenges. We introduced a family of new *Metric-Chisini-Jensen-Shannon divergences (M-CJDs)* based kernels, namely, *Amplified, Scaled, Amplified-Scaled.* We proved a number of mathematical properties, developed an information theoretic method for the measurement of car occupancy rates at parking lots during the weekdays, developed an optimization approach to modify k-Means clustering by transforming L^2-distances between data points.

Viability of pig tissue and tACS as a testbed for EEG systems

Sinks, C.[1]*, Nonte, M.*[1] *and Hairston, W.D.*[1]

[1]CCDC Army Research Laboratory, **FCDD-RLH-FA**, APG, MD

*corresp. author: christopher.sinks.ctr@mail.mil

Electroencephalogram (EEG) systems commonly used in laboratory environments are rapidly moving towards real-world applications. However, extracting EEG data from noise in ecologically valid environments presents unique challenges. Accurately classifying the noise associated with variable environments requires a known signal, which is quite difficult for intact-human brain signals. Our solution is to inject a known, EEG-like signal into the live human scalp using a custom transcranial alternating current stimulator (tACS). The objective of this study was to validate the approach prior to use on human subjects. Pig tissue is a known analog for human tissue, thus we used pig skin and whole pig heads to simulate passive human tissue properties. We used the custom tACS to inject a chirp signal on the pig scalp, and measured that signal both within the cranial cavity and at various points on the scalp. With this validation, we plan to move forward into using a live human with EEG level signals injected at the scalp to accurately reproduce environmental and task-related noise with a ground-truth signal which will allow for accurate noise classification.

Acoustic Wireless Power Transfer

Tseng, V.[1]*, Drummond, T.*[1]*, Lazarus, N.*[1] *and Bedair, S.*[1]

[1]CCDC Army Research Laboratory, **FCDD-RLS-CC**, Adelphi, MD

*corresp. author: victorfarm-guoo.tseng.civ@mail.mil

ARL has been investing in the R&D of wireless power transfer (WPT), which can be used to alleviate the current soldier battery burden by automatically powering soldier equipment, UAV's, and embedded sensors for vehicle structural health monitoring (SHM). In particular, our work has been on developing acoustic WPT for through-air and through-metal applications. We have experimentally verified that acoustic WPT can achieve higher power transfer efficiencies than conventional inductive WPT when the transfer distance is above several times the diameter of the coils/transducers, which is due to the shorter acoustic wavelengths, allowing it to be beamformed much easier at lower frequencies. For our work on through-air acoustic WPT, we demonstrated for the first time, the feasibility of using an acoustic phased array transmitter to achieve power beaming. With a 37 element 40 kHz array, we demonstrated the ability to focus acoustic waves to a single focal point to transfer power to selected locations, while emitting minimal external detectable signatures. Critical factors to increase efficiency and provide higher power were also investigated. A unique advantage of acoustic waves is that it can propagate through metal, while electromagnetic waves (used in all other forms of WPT) are blocked by metal barriers due to Faraday shielding. Therefore, it is possible to achieve through-metal transfer with acoustic waves. We have demonstrated acoustic power/data transfer to a wireless sensor node embedded within metal for SHM. The power received at the node is temporarily stored, then used to acquire and back transmit sensor information. The node was packaged within a compact size, and entirely embedded within a casted metal cube to demonstrate its functionality. The measured results corresponded well with modeling, achieving a peak power transfer efficiency of 33% at 440 kHz. Instead of transferring power through the "thickness" of a metal wall, power can also be transferred along the "length" of a metal plate by using guided plate waves (Lamb waves), achieving longer distance transfer due to the lower attenuation. This can be used to power sensors attached to airplane wings, pipelines, etc.. For this area, we have currently demonstrated up to 40-60% power transfer efficiency at a 40-50 cm distance along metal plates and tubes.

Topologically Enabled Devices: α-Sn Magnetotransport

Vail, O.[1]*, Taylor, P.*[1]*, Folkes, P.*[1]*, de Coster, G.*[1]*, Beck, W.*[1] *and Jankowski, N.*[1]

[1]CCDC Army Research Laboratory, **FCDD-RLS-EE**, Adelphi, MD

*corresp. author: owen.a.vail.civ@mail.mil

The diamond-cubic phase of Tin known as α-Sn is of significant scientific interest due to its topological band structure and single-element nature. Consistent high-quality growth on insulating CdTe opens the doors to unconventional electronics using a widely available material. After verifying epitaxial growth of our films, we perform transport measurements to characterize the electronic carriers in the material. We identify two-channel transport with n-type and p-type intrinsic carriers that shifts as a function of thickness. We attribute the n-type transport to a semimetallic channel that tentatively suggests Dirac behavior, and the p-type transport to growth impurities resulting from the CdTe substrate. We apply a field effect gate voltage in order to map out the charge neutrality point and reveal a distinct modulation between high mobility n-type carriers and low mobility p-type carriers. Careful preparation of the CdTe surface before growth is considered crucial to attain a low dopant density and accessible topological states on an insulating substrate. This work readily lends itself to the development of topologically enabled devices for Army applications such as low power electronics in order to achieve advanced computing at the edge and a reduced logistics tail for military operations.

Tunable and tailorable thermal properties of solid-state materials

Wilson, A.A.[1]*, Sharar, D.J.*[1]*, Leff, A.*[2]*, Brody, J.*[1,3] *and Wright, J.*[1,4]

[1]CCDC Army Research Laboratory, **FCDD-RLS-DP**, Adelphi, MD, [2]CDC Army Research Laboratory, **FCDD-RLS-DE**, Adelphi, MD, [3]Department of Materials Science, University of Maryland, College Park, MD, [4]Department of Materials Science, University of Pittsburgh, Pittsburgh, PA

*corresp. author: adam.a.wilson6.civ@mail.mil

Thermal conductivity is conventionally thought of as an intrinsic material property, and not easily tunable. In this work, we demonstrate strategies to tune thermal conductivity by external stimuli over a significant range (up to a factor of two). By understanding and manipulating the underlying mechanisms for scattering of thermal energy carriers, the effective value of thermal conductivity in materials and devices may also be tailor-made for specific applications. To demonstrate these strategies, we characterize thermal conductivity as a function of temperature for solid-solid phase change materials such as NiTi and NiTiCu, where we carefully tailor defect density by heat-treating over a variety of precipitate growth conditions. Across the phase transition, the crystal lattice shifts, thereby changing the phonon density of states, and subsequent phonon scattering, leading to a significant change in thermal conductivity (going from less than 10 $Wm^{-1}K^{-1}$ to more than 20 $Wm^{-1}K^{-1}$). The ability to tailor and tune thermal properties is critical for Army needs, as the Army moves more towards several high-priority technologies. These include 1) High energy-density and directed energy applications (where high electrical current density means extremely high heat flux generation which may cause thermally-driven failure of electronics of advanced optics), 2) Computation at the edge (where on-demand changes in thermal properties can allow for passive feedback and computation that does not require any on-board power) and 3) Machine (and soldier-borne) vision in infrared (where the ability to tailor and tune thermal properties can enhance sensitivity of next-generation IR detectors and provide enhancement in significant dynamic range).

Development of Protein Catalyzed Capture Agents for the Detection of E. coli O157:H7 in Food

Winton, A.[1]*, Ngo, A.*[1] *and Coppock, M.*[1]

[1]CCDC Army Research Laboratory, **FCDD-RLS-EB**, Adelphi, MD

*corresp. author: alexander.j.winton2.civ@mail.mil

Foodborne pathogens represent a significant health concern worldwide with the World Health Organization estimating 582 million illnesses annually. The enterohemorrhagic E. coli (EHEC) O157:H7 is of particular interest, attributing to more than 3,600 illnesses in the US each year. Ensuring food safety is pertinent to Army operations. Current culture based detection methods are slow and fail to detect contamination in real-time. Newer assays utilizing E. coli specific antibodies to capture and concentrate target bacteria have demonstrated improved detection times and limits. The use of antibodies as a target recognition element represents the current gold standard as they exhibit target specificity and excellent binding affinities however, they are costly, labor intensive to produce, and have limited storage shipping capabilities. Peptides provide an advantageous alternative to antibodies as they exhibit improved storage and shelf-life capabilities, are inexpensively generated by chemical synthesis, and can incorporate unnatural chemistries. This work seeks to identify E. coli O157:H7 specific peptide affinity ligands, developed through the protein catalyzed capture (PCC) agent method, for detecting pathogen contaminated food and beverages. A One Bead-One Compound (OBOC) cyclic peptide library is screened against synthetic peptide epitopes (SynEps) derived from unstructured, solvent exposed domains of intimin, a protein target of interest. Library "hits" are generated in situ by uncatalyzed, entropically favored "click" reactions between alkyne and azide functional handles located on the library's cyclic peptide and SynEps respectively. Magnetic beads will be functionalized with designed multi-valent peptide constructs to enable E. coli separation and subsequent detection from bulk food samples.

Appendix B. Contributed Posters Presented at the 4th Postdoc and Early Career Research Day

REFLECT: A Methodology for Capturing Team Communication Flow in Real-Time

Anthony L. Baker, Ralph W. Brewer, Susan G. Hill, & Kristin E. Schaefer
U.S. Army CCDC Army Research Laboratory

Summary: This poster details the development and initial usability assessment of the Realtime Flow, Event, and Coordination Tool (REFLECT). This methodology provides an approach to capture team communication flow in real-time to support the development of effective metrics and interventions that can be used to enhance team trust and team cohesion (directly supporting the Human-Autonomy Teaming Essential Research Program). It is critical to human-autonomy teaming because communication is integral to developing team processes for synchronizing information from multiple sources, aligning goals, distributing critical information, and resolving issues, leading to effective performance.

REFLECT User Interface

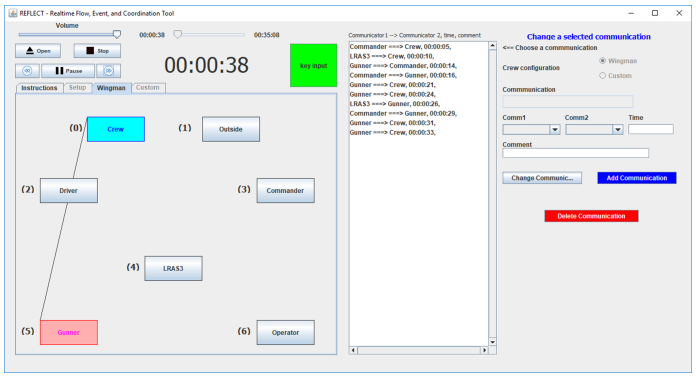

Usability Assessment

Participants. Four participants from ARL workforce.

Task. Used REFLECT to assess the coordination and communication of a 5-man human-autonomy team during a mounted machine gun live fire exercise collected as part of the US Army Wingman JCTD field exercise at Ft Benning, GA, October 2018.

Pre-task training. Participants were trained for 30 minutes to familiarize with the crews' voices, the gunnery exercise in the audio recording, and REFLECT.

Results

Performance. Participants reached accuracy between 61-75% when identifying senders and receivers.

Real-time. Participants averaged between 1.35 and 2.48 s between hearing a communication event and logging in REFLECT.

	P1	P2	P3	P4
Accuracy	74.6%	71.7%	61.2%	74.6%
Lag Time (s)	1.99	1.35	2.48	2.13

Overall	Mean	Std Dev
Accuracy	70.5%	6.3%
Lag Time (s)	1.99	0.47

Usability perceptions. Participants rated perceptions of different aspects of REFLECT and the real-time coding methodology.

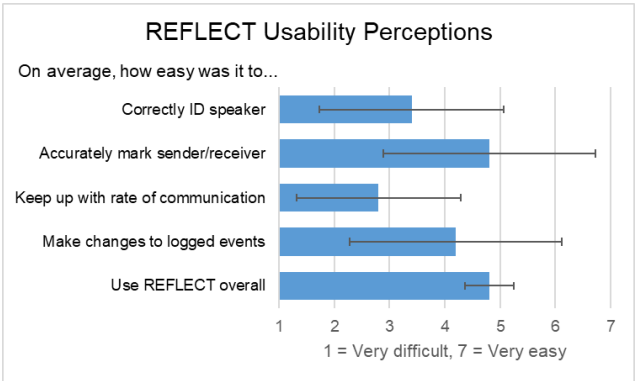

Requested improvements. Add hotkeys, allow rearrangement of roles on the user interface, improve fast forward/rewind abilities, improve error correction speed.

Insights. To code accurately, quickly, and reliably, users must become familiar with:

- **Voices:** Must distinguish team members in order to code accurately
- **Task context:** Must understand team's tasks to infer senders and receivers based on speech
- **Unitizing:** Must train to become consistent in dividing speech into discrete units

Sender	Receiv.	Time
VC	Crew	6:34
LRAS	Crew	6:38
VC	LRAS	6:41
RVG	VC	6:42
VC	RVG	6:43
RVG	VC	6:44
LRAS	Crew	6:48

Example REFLECT output

Path forward. Add requested improvements and conduct follow-on test. Explore algorithmic logging of senders/receivers to supplement or replace human observations.

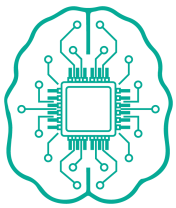

- Receive input from event loggers and other technology sources to automate identification of senders/ receivers
- Context will be important for accurately identifying receivers. Need to explore how context can be integrated and processed quickly by humans and future algorithms
- Investigate AI/machine learning applications for communication pattern analysis

This research was supported in part by an appointment to the US Army Research Postdoctoral Fellowship Program administered by the Oak Ridge Associated Universities through a cooperative agreement with the US Army Research Laboratory (ARL). Research was sponsored by ARL and was accomplished under Cooperative Agreement Number W911NF-18-2-0230

Partial synchrony and chimera states in human brain networks

Kanika Bansal[1,2], Javier O. Garcia[1,3], and Jean M. Vettel[1,3,4]

[1]U.S. CCDC Army Research Laboratory, Aberdeen Proving Ground, MD; [2]Department of Biomedical Engineering, Columbia University, New York, NY; [3]Department of Bioengineering, University of Pennsylvania, Philadelphia, PA; [4]Department of Psychological and Brain Sciences, University of California, Santa Barbara, CA.

Abstract

Partial synchronization is ubiquitous to the dynamics of complex real-world systems. The human brain, a complex biological system, functions through the emergence of coherent and incoherent activity between distributed neuronal components. This activity balances the segregation of information for localized processing while also maintaining efficient integration of information for global coordination. Human cognition relies on the states of partial synchrony, including chimera states with separate domains of synchronized and de-synchronized dynamics. We propose that spatial patterning of these partial synchrony states plays a fundamental role in individual variability in cognitive performance. In our recent paper (Bansal et al. 2019, Sci Adv), we used a chimera-based framework to capture individual differences in structurally-constrained computational models of the brain. Our ongoing research extends this work from individual brains to team performance.

Analysis framework

Personalized brain network models[1,2]

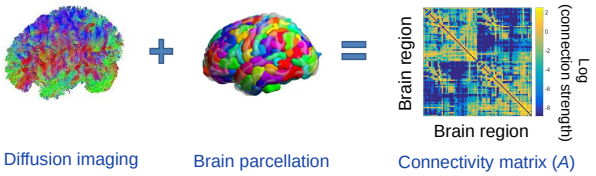

Diffusion imaging | Brain parcellation | Connectivity matrix (*A*)

Excitatory population

$$\tau\frac{dE_i}{dt} = -E_i(t) + \left(S_{E_m} - E_i(t)\right)S_E\left(c_1E_i(t) - c_2I_i(t) + c_5\sum_j A_{ij}E_j\left(t-\tau_d^j\right) + P_i\right) + \sigma w_i(t)$$

Excitatory coupling term | External Stimuli | Noise

Inhibitory population

$$\tau\frac{dI_i}{dt} = -I_i(t) + \left(S_{I_m} - I_i(t)\right)S_I\left(c_3E_i(t) - c_4I_i(t) + c_6\sum_j A_{ij}I_j\left(t-\tau_d^j\right)\right) + \sigma v_i(t)$$

Inhibitory coupling term

where

$$S_{E,I}(x) = \frac{1}{1+e^{\left(-a_{E,I}(x-\theta_{E,I})\right)}} - \frac{1}{1+e^{a_{E,I}\theta_{E,I}}}$$

$\tau = 8$, $c_1 = 16$, $c_2 = 12$, $c_3 = 15$, $c_4 = 3$, $\sigma = 10^{-5}$, $a_E = 1.3$, $a_I = 2$, $\theta_E = 4$, $\theta_I = 3.7$

Subject dependent coupling parameter

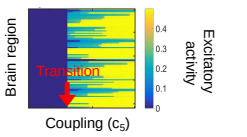

Emergent dynamical states upon regional stimulation

Cognitive systems[3]

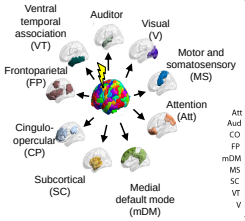

Synchrony: measured through order parameter ρ, defined as[4]

$$\rho(t)e^{i\varphi(t)} = \frac{1}{N}\sum_{j=1}^{N} e^{i\theta_j(t)}$$

N: number of oscillators
$\theta_j(t)$: phase of the j^{th} oscillator at time *t*.

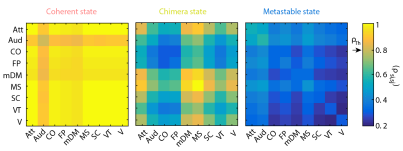

Main results: characteristics of emergent states

Spatially distributed nodes produce different states

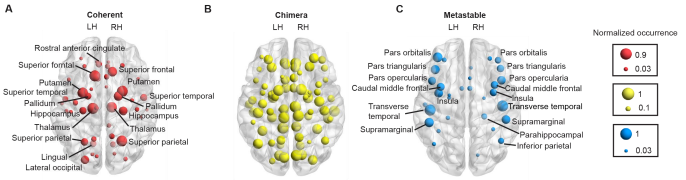

Prevalent patterns within cognitive systems

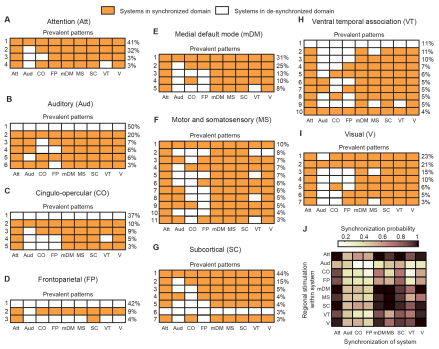

- Attention, medial default mode, subcortical, and visual systems are dominated by highly synchronized patterns.
- Auditory, frontoparietal, and cingulo-opercular systems produce diverse set of patterns, dominated by a metastable state.
- Motor and somatosensory and ventral temporal association systems show a large number of patterns, with no specific dominance.

Patterns robustness

Similarity of emergent patterns produced by a given system, across subjects and across regions within.

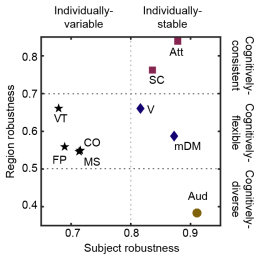

Conclusions

- We present a chimera-based, cognitively-informed analysis framework to assess within and between individuals variability in structural and functional brain networks.
- Our results indicate characteristically different levels of subject-specific and region-specific structural variability across cognitive systems within the brain, which represent the functional role a cognitive system serves.
- This approach can be extended to assess variability of functional patterns within an individual, across different individuals during task performance, as well as between individuals during team interactions.

References

1. Wilson HR, Cowan JD, Excitatory and inhibitory interactions in localized populations of model neurons, *Biophysj*. 1972,**12**(1):1–24.
2. Muldoon SF et al. Stimulation-based control of dynamic brain networks, *PLoS Comput Biol.* 2016,**12**(9): e1005076.
3. Power JD et al. Functional network organization of the human brain, *Neuron,* 2011, **72**, 665–678
4. Kuramoto Y, Chemical oscillations, waves, and turbulence, Springer- Verlag, Berlin, 1984.

Acknowledgment

This work was supported by the U.S. CCDC Army Research Laboratory through contract # W911NF-16-2-0158 from the U.S. Army research office. The content is solely the responsibility of the authors and does not necessarily represent the official views of the funding agency.

High-Pressure Characterization of High-Performance Insensitive Energetic Materials: Dihydroxylammonium 5,5'-Bis(3-Nitro-1,2,4-Triazolate-1N-Oxide) (MAD-X1)

Jonathan C. Bennion, FCDD-RLW-LB, jonathan.c.bennion.ctr@mail.mil
Jennifer A. Ciezak-Jenkins, Timothy A. Jenkins

Abstract

The high-pressure behavior of dihydroxylammonium 5,5'-bis(3-nitro-1,2,4-triazolate-1N-oxide) (MAD-X1) was studied at room temperature to 25 GPa by Raman spectroscopy and powder X-ray diffraction. No evidence of polymorphism was observed over this pressure range, indicating that the ambient structure of MAD-X1 remains stable up to conditions similar to the detonation pressure of the material. Additionally, such findings suggest that this high performance material can serve as an insensitive RDX replacement in energetic formulations without the concern of uncontrolled polymorphism that might otherwise affect the performance and safety of the munition.

Introduction and Background

- The desire for insensitive high performance explosives remains a central goal driving synthetic efforts in energetic materials research over the past decades
- The Klapötke group at the University of Munich recently investigated the salt formation of DNBT N-oxide derivatives and discovered several promising bis-1,2,4-triazoles materials
  - Dihydroxylammonium 5,5'-bis(3-nitro-1,2,4-triazolate-1N-oxide) (MAD-X1) shows the most promise for explosive applications

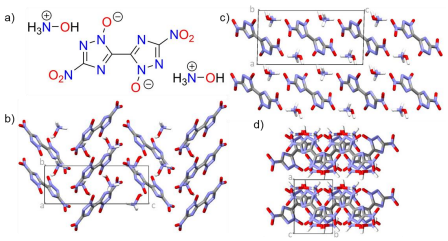

	MAD-X1
Space Group	$P2_1/c$
a (Å)	7.307
b (Å)	5.243
c (Å)	14.403
β (°)	91.498
Volume (Å³)	551.61
Z	2
Density (g/cm3) At 298 K	1.90

- MAD-X1 possess favorable energetic properties for insensitive explosives applications:
  - High crystallographic density (1.90 g/cm³)
  - Detonation velocities of 9158 m/s
  - Detonation pressures of 41.2 Gpa
  - Impact and friction sensitivity of >40 J and >360 N, respectively

Experimental

- Diamond anvil cells (300 µm) with rhenium gaskets and ruby and Au pressure markers
- Raman Spectroscopy with 532 nm cw laser in a backscattering geometry
- X-ray diffraction at ALS Beamline 12.2.2

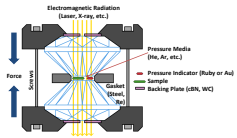

Results – Raman Spectroscopy

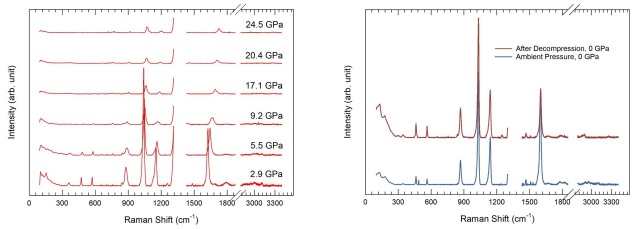

Pressure Dependence of Raman Peaks

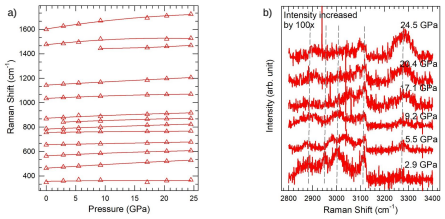

- Spectra match well with previously reported vibrational spectra
- All vibrational modes showed nearly linear slopes with increasing pressure, suggesting no phase change
- Blue shifts above 5.5 GPa are consistent with strong hydrogen bonds or those that are confined as a result of pressure

Acknowledgments

Dr. T. M. Klapötke is thanked for providing the MAD-X1. Portions of this work were performed at the Advanced Light Source, which is supported by the Director, Office of Science, Office of Basic Energy Sciences, of the U.S. Department of Energy under Contract No. DE-AC02-05CH11231.

Results - Powder X-ray Diffraction

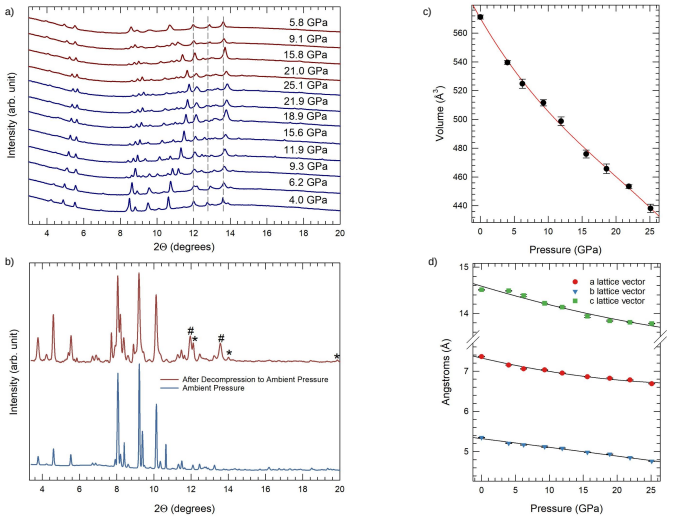

- MAD-X1 undergoes smooth compression, with no evidence of a phase change
  - Peak broadening is consistent with gradual stress-induced amorphization
- The isothermal bulk modulus (B_o) and its pressure derivative (B') were determined from fitting the P-V to a third-order Birch-Murnaghan equation of state to near 25 GPa
  - B_0 = 70.5 ± 3.9 GPa and B' = 2.8 ± 0.34
- Over the experiment, the crystal lattice experiences a total volume compression of 23.3%
  - Low compressibility likely a result of the high degree of hydrogen bonding associated with insensitive materials
- The *b*-axis is the most compressible axis – (10.9%)
  - Corresponds to the slip plane of the stacks of linear tapes and likely results in an alteration π interactions between adjacent molecules of the N-oxide anion and the hydroxylammonium cations
- The *c*-axis is the least compressible axis – (5.1%)
  - Corresponds to the compression of the herringbone packing of the molecules of MAD-X1

Conclusions

- High-pressure behavior of MAD-X1 was examined to pressures exceeding 25 GPa
  - Via both Raman spectroscopy and powder X-ray diffraction
- Ambient pressure monoclinic crystallographic structure of the material remained stable under hydrostatic compression
  - Findings suggest that this high performance material can serve as an insensitive RDX replacement in energetic formulations
- No evidence of high-pressure polymorphism over the pressure range
  - Insensitivity of MAD-X1 is associated with the high degree of intermolecular hydrogen bonding between the two components of the salt
- Values for the isothermal bulk modulus (B_0) and its pressure derivative (B') were determined and are similar to that of other heterocyclic energetic molecules
  - Provides theorists with valuable thermodynamic information, that is essential to accurately predicting the performance properties of a novel energetic

References

1. Klapötke, T. M., *Chemistry of High-Energy Materials*. 3 ed.; Walter de Gruyter: Berlin/Boston, **2015**.
2. A. A. Dippold, T. M. Klapötke,, *J. Am. Chem. Soc.*, **2013**, *135*, 9931-9938.
3. Meyer, R.; Köhler, J.; Homburg, A., *Explosives*. Wiley-VCH Verlag GmbH & Co. KGaA: **2003**; pp 307-360.
4. J. Sabatini, K. Oyler, Recent Advances in the Synthesis of High Explosive Materials, *Crystals*, **2016**, *6*, 5.
5. J. C. Bennion, A. McBain, S. F. Son, A. J. Matzger, *Cryst. Growth Des.*, **2015**, *15*, 2545-2549.
6. A. A. Dippold, T. M. Klapötke, Nitrogen-Rich Bis-1,2,4-triazoles—A Comparative Study of Structural and Energetic Properties, *Chem. Eur. J.*, **2012**, *18*, 16742-16753.
7. P. F. Pagoria, G. S. Lee, A. R. Mitchell, R. D. Schmidt, A review of energetic materials synthesis, *Thermochim. Acta*, **2002**, *384*, 187-204.

THE ATTENTIONAL DRAG: HOW FEATURE TEMPORAL AUTOCORRELATION AND VISUAL TRANSIENTS EXTEND AND CLOSE ATTENTIONAL WINDOWS IN TIME.

Chloe Callahan-Flintoft, ORAU

Supported by NSF Grant BCS-1331073

Motivation

- To optimize visual search for soldiers with technologies such as AR, we need to understand how the visual system samples information from the environment.

How fast does the visual system extract information in time?

- Presenting discrete stimuli we find near-zero (< 25 ms) latencies[1,2]
- But when features change smoothly, *extraction can be as late as 400 ms*[3,4]

Exp 1: Does smooth feature change increase selection latency?

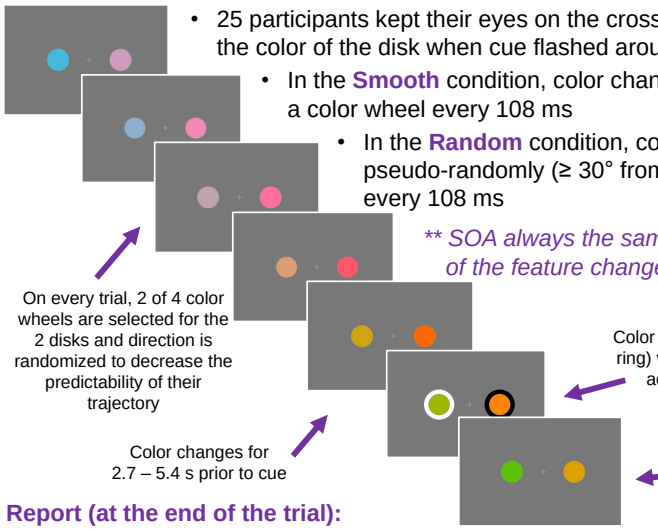

- 25 participants kept their eyes on the cross and reported the color of the disk when cue flashed around it
  - In the **Smooth** condition, color changes 16° around a color wheel every 108 ms
  - In the **Random** condition, color changes pseudo-randomly (≥ 30° from previous color) every 108 ms

*** SOA always the same but the nature of the feature change is different ***

Report (at the end of the trial):

Participants move mouse horizontally to change the color of the test disk to match their memory

- All data analyzed using a permutation analysis

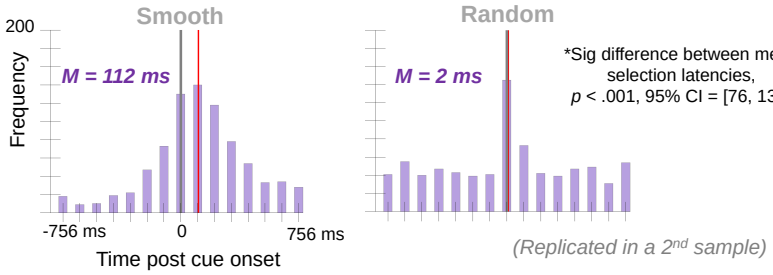

Smooth feature change increases selection latency. Could be that activating overlapping neural representations sequentially (i.e smooth presentation) maintains attentional engagement.

Exp 2: Does increasing the smoothness increase the selection latency?

- 25 participants complete same task as Exp 1
- In the **Smoother** condition color changes 4° / 27 ms. In the **Smooth** condition color changes 16° / 108 ms (same as Smooth condition of Exp 1)

*** Rate of change is the same in both conditions***

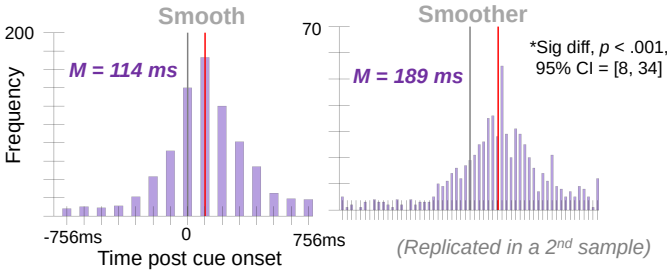

Increasing the smoothness increases selection latency. But this could also be a seen as an increase in predictability.

Exp 3: Is the increase in selection latency due to the increase in predictability of the trajectory?

- 20 participants complete same task as Exp 1

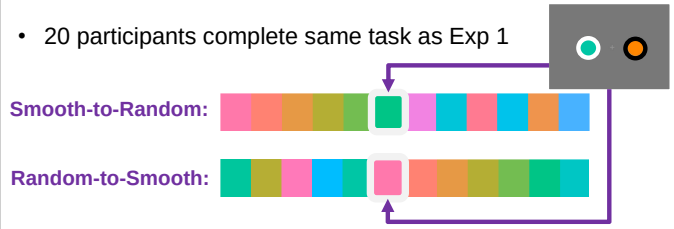

*** Only temporal autocorrelation changes after cue, not SOA (108 ms)***

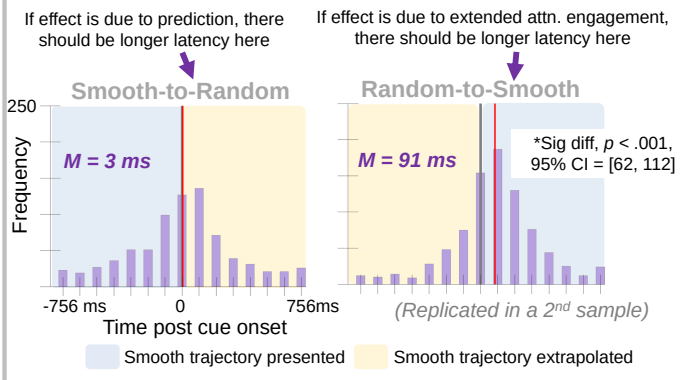

Only temporal autocorrelation presented after the cue, not before, increases selection latency.

Attentional drag model

- A proposed neural circuitry that accounts for how smooth feature change extends attentional engagement while a feature transient will cause rapid disengagement

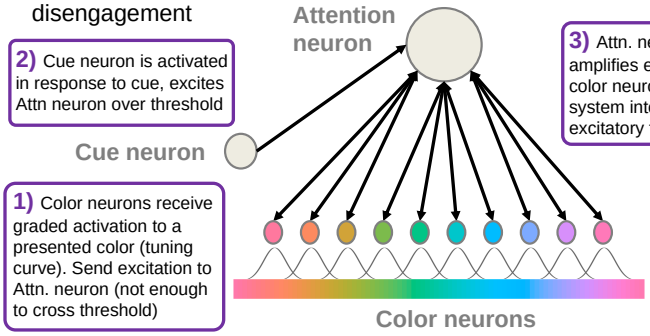

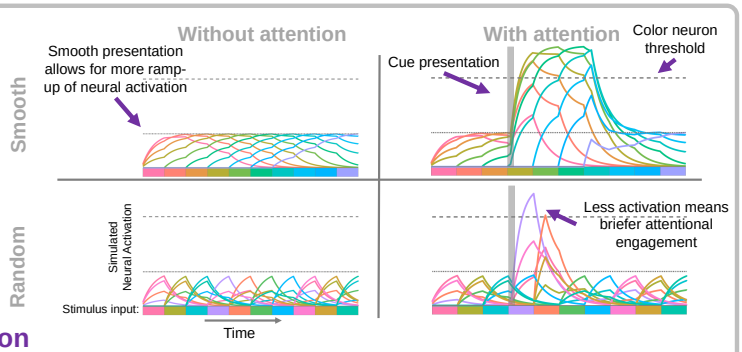

Conclusion

- Attn. sampling differs depending on how features are changing in time
- Temporal autocorrelation could be how the brain parses continuous input into meaningful episodes and constructs coherent object representations

[1]Goodbourn, P. T., & Holcombe, A. O. (2015). "Pseudoextinction": Asymmetries in simultaneous attentional selection. *JEP: HPP, 41*(2)
[2]Vul, E., Nieuwenstein, M., & Kanwisher, N. (2008). Temporal selection is suppressed, delayed, and diffused during the attentional blink. *Psych Sci, 19*(1)
[3]Carlson, T. A., Hogendoorn, H., & Verstraten, F. A. (2006). The speed of visual attention: What time is it?. *Journal of Vision*, 6(12)
[4]Sheth, B. R., Nijhawan, R., & Shimojo, S. (2000). Changing objects lead briefly flashed ones. *Nature Neuro*, 3(5)

The use of hydrogen in titanium additive manufacturing

Matt Dunstan, Brady Butler, & James Paramore

Objectives

- Reduce the cost of titanium additive manufacturing
- Improve reliability of additively manufactured Ti-6Al-4V components

Approach

Use hydrogen as a temporary alloying element to increase densification kinetics (reduce porosity), refine microstructure, and improve performance of titanium alloys.

Based on established powder metallurgy technique called Hydrogen Sintering & Phase Transformation (HSPT).

Two methods:

1. Low-Cost Fused Filament Fabrication (FFF)
   - Produce a Ti-6Al-4V – hydride loaded filament and print using a cheap plastic 3D printer.
   - Debind and sinter in hydrogen to produce a densified, ultra-fine grained Ti-6Al-4V part.
2. Thermo-Hydrogen Grain Refinement (THRM)
   - Heat treat Ti-6Al-4V made via beam based AM techniques (e.g. SLM, DED, EBM) under controlled hydrogen atmosphere

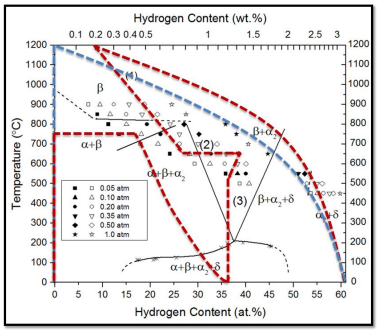

(Ti-6Al-4V)-H phase diagram

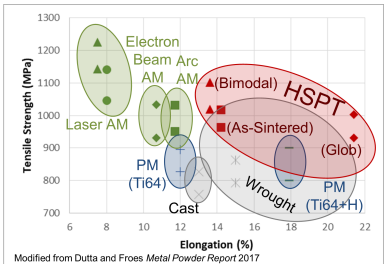

Comparison of HSPT mechanical properties to other manufacturing processes

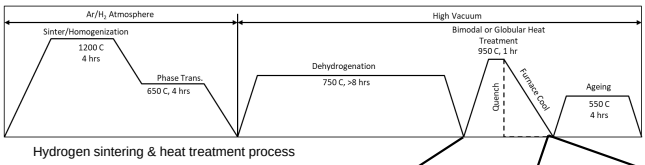

Hydrogen sintering & heat treatment process

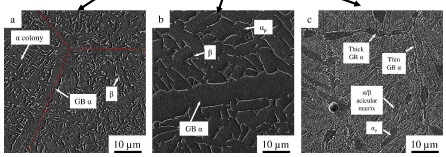

Possible microstructures from hydrogen sintering/heat treatment

Results

1) FFF

- Developed flexible & durable filament
- Printed & sintered test pieces
- Relative densities >90% possible
- Filament processing temperatures are too high causing interstitial contamination from polymer burning

Flexible (Ti-6Al-4V)-H filament

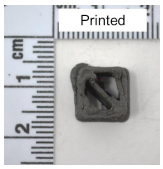

Printed filament

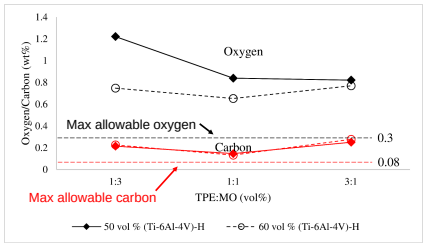

Oxygen & carbon content

2) THRM

- Developed versatile process for treatment of Ti-6Al-4V from various processing methodologies: Additive manufacturing (e.g. DMLS/SLM, EBM, DED, WAAM, etc), traditional powder metallurgy, cast and wrought processing.
- Resets unfavorable microstructures
- Tunable hydrogen processing treatments
- Reduce porosity, refines microstructure, minimizes anisotropy, & improves mechanical properties

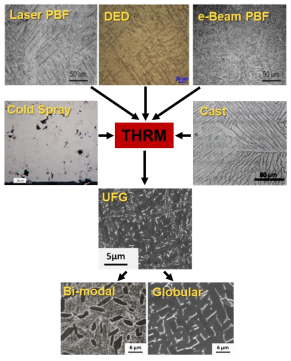

THRM effects on microstructure

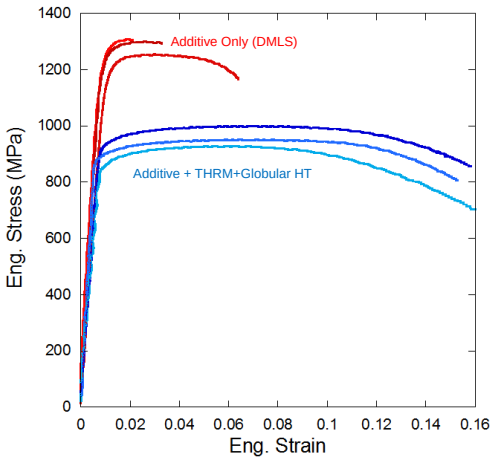

THRM effects on tensile properties

Summary

- Hydrogen can be used to improve titanium additive manufacturing through low-cost FFF or as a post-AM heat treatment
- FFF has many engineering hurdles preventing adoption – currently collaborating with industry partners
- THRM can reset unfavorable microstructures and improve the microstructure & mechanical properties

High Strain Rate Behavior of Medium-Mn TRIP Steel

PURPOSE

Determine if new TRIP steels can be designed for ballistic applications outside the designed target of commercial automotive

BACKGROUND

- Two-stage TRIP steels are unique class of alloy systems under investigation.
  - Strength of medium carbon quench & tempered steels
  - Work hardening of austenitic stainless steels
- Microstructures are tri-phase
  - γ-austenite (fcc), ε-martensite (hcp), α-martensite (bcc)
  - Two sequential transformations are activated during deformation
    - Stage I: $\gamma \rightarrow \varepsilon$ ($\Delta V < 0$)
    - Stage II: $\varepsilon \rightarrow \alpha$ ($\Delta V > 0$)
- Two-stage TRIP behavior is controlled by Stacking Fault Energy (SFE)

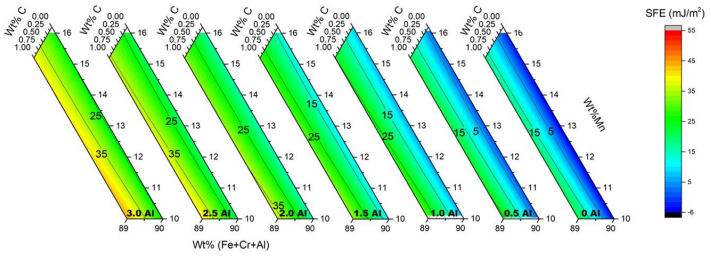

Figure. Stacking Fault energy as a function of C, Mn, and Al with fixed Si (1.0 wt.%) and N (0.007 wt.%) contents

PROCEDURE

- Hot roll at 1000 °C (1832 °F) and anneal two TRIP steels at 650 °C (1200 °F)
- Electron Backscattered Diffraction (EBSD)
- Split Hopkinson Pressure Bar testing
  - Determine high strain rate flow stress

Table. Compositions of the TRIP steels investigated

	Composition (wt%)				
	C	Mn	Si	Al	SFE
Alloy 1	0.17	10.6	2.08	1.54	11.3
Alloy 2	0.15	10.2	2.07	0.71	3.0

MICROSTRUCTURE

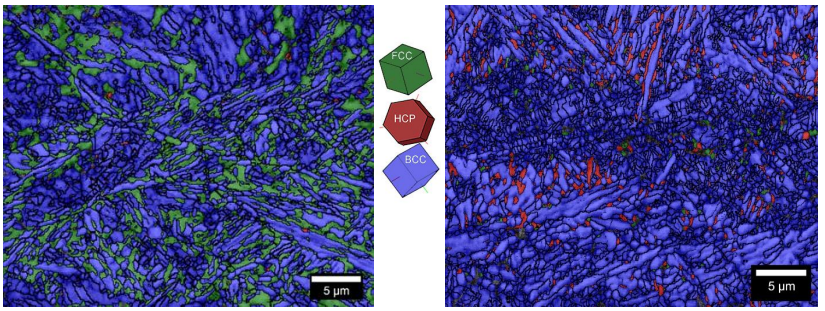

Figure. EBSD Phase map of Alloy 1 (left) and Alloy 2 (right).

Table. Microstructure of Alloys

	Vol % Phase		
	γ	ε	α
Alloy 1	21	6	73
Alloy 2	9	24	67

- Alloy 1: Stage I TRIP ($\gamma \rightarrow \varepsilon$ $\Delta V < 0$)
- Alloy 2 Stage II TRIP ($\varepsilon \rightarrow \alpha$ $\Delta V > 0$)

MECHANICAL PROPERTIES

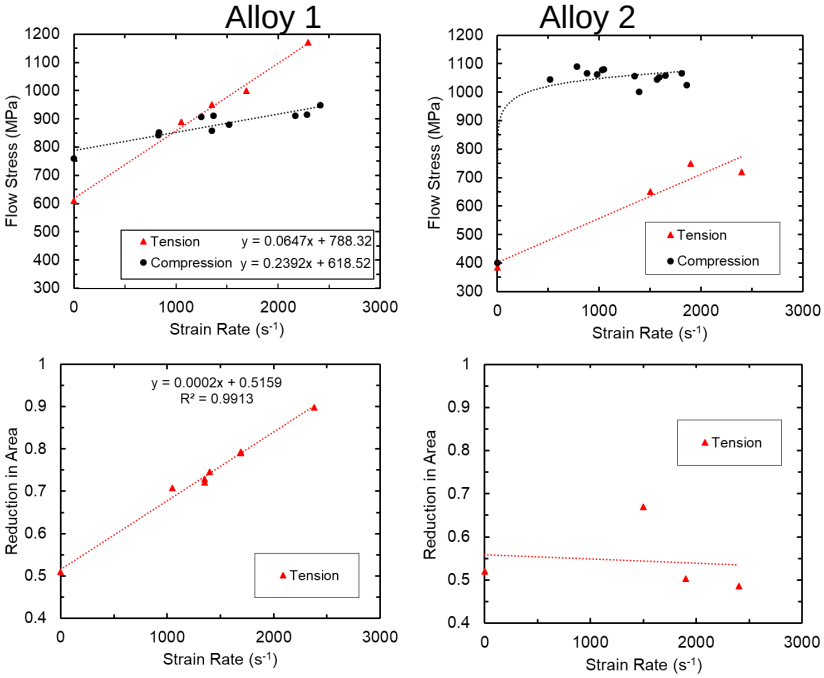

Figure. High strain rate properties of the developed alloys. Both steels exhibit positive strain rate response for strength

CONCLUSION/FUTURE WORK

- Alloys containing γ-austenite in starting structure had higher flow stress in tension than alloy containing ε-martensite.
  - Opposite was observed in compression.
- Response is rationalized upon volume transformation during TRIP reactions: $\gamma \rightarrow \varepsilon$ ($\Delta V<0$) or $\varepsilon \rightarrow \alpha$ ($\Delta V>0$)
- Determine ballistic performance of material under complex stress state for armor application

POINT OF CONTACT: Daniel M. Field Ph.D
Daniel.field8.ctr@mail.mil
410-306-0742

AT-CUT QUARTZ PIEZOELECTRIC TRANSFORMERS FOR PASSIVE VOLTAGE GAIN IN AN RF FRONT-END

Mary Beth Galanko, mary.e.galanko.ctr@mail.mil
Sarah S. Bedair, Ryan Rudy*, Victor F.-G. Tseng, Jeffrey S. Pulskamp*, Iain Kierzewski

Sensors and Electron Devices Directorate
Energy & Power Division, Power Components Branch (FCDD-RLS-DE)
*Electronics & RF Division, Micro & Nano Materials & Devices Branch (FCDD-RLS-RL)

Objective:

Provide the Army with near-zero-power "wake-up" radios that **monitor contested environments** for RF signals, continuously for a period of months to years, **without the need to replace a battery**.

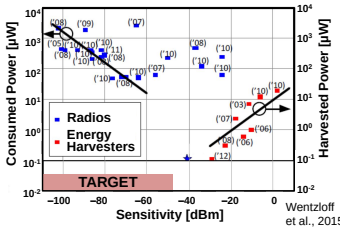

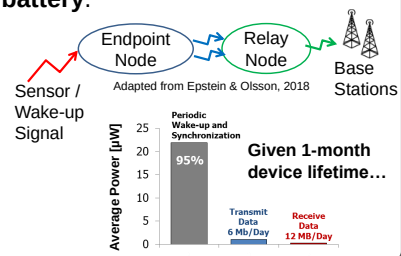

Approach:

Explore quartz as a material for low-power piezoelectric transformers (PTs)

- Investigate achievable **passive voltage gain, quality factor (*Q*), and matching** to 50 Ω
- Explore advantages of "stacking" multiple quartz substrates
- Integrate with state-of-the-art circuit with power consumption **<10 nW** for sensitivity approaching **–100 dBm**

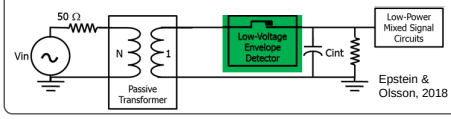

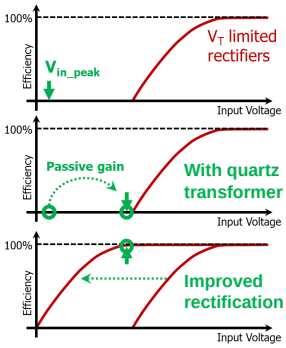

Voltage Gain Testbed

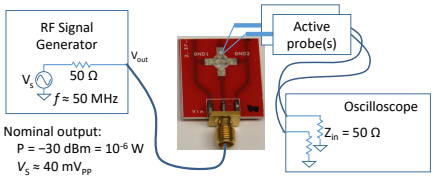

Active probe setup:

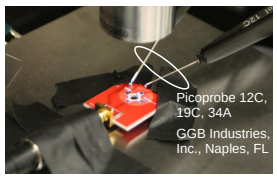

Single-substrate Resonator Measurements

- **1-port resonator screening:**
  - Measure distribution in *Q*, f_r, etc.
  - Wide variation:
    Q ≈ 20000-140000
    V_{out} / V_S ≈ 15-115 V/V

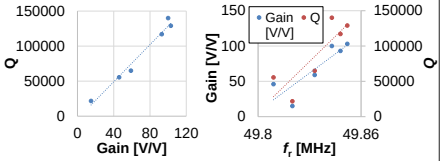

- **2-port PT screening:**
  - 22 devices tested
  - At any given *Q*, gain varies widely:
    V_{out} / V_S ≈ 18-100 V/V, **avg = 62 V/V**
    Standard deviation = 18 V/V
    Consistent with analysis of df

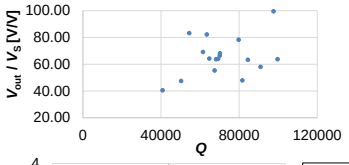

- **Highest measured 2-port PT gain:**
  - **Gain = 99.5 V/V** (to 50 Ω)
  - **Q = 97627**
    - *Note: not necessarily max Q = max gain*

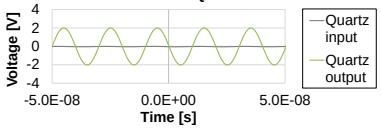

Piezoelectric Transformer Design

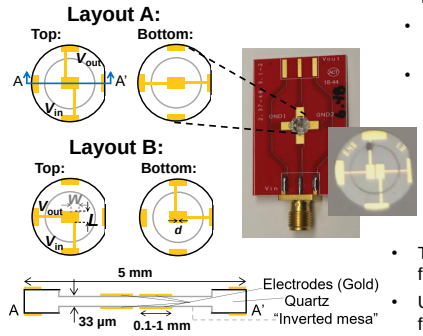

- Excite quartz in **thickness-shear** mode
- Leverage **high *Q*** – high voltage gain & out-of-band rejection
- Utilize **energy trapping** – excite at *ω* between cutoff frequencies ω_e & ω_s:

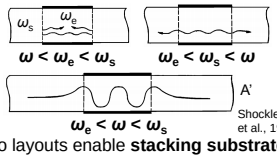

- Two layouts enable **stacking substrates** for parallel input, series output **(PISOT)**
- Use **commercially available** quartz fabrication process

Compare with PISOT Measurements

- N = 2 yields **17% gain increase** for high-Z load
- **Matching** to 50 Ω improves:
- **Gain increase** consistently observed for **low-Z loads**

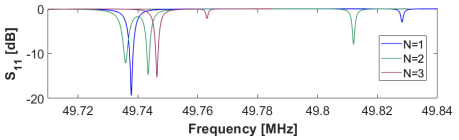

Representative gains measured in PISOT vs. single-substrate:

Device	f_r [MHz]	Load = 20 fF || >>1 GΩ Q_{elec} >> 100		Load = 120 fF || 1 MΩ Q_{elec} ≈ 37.7		Load = 100 fF || 1 MΩ Q_{elec} ≈ 31.4	
		V_{out}/V_S [V/V]	*Q*	V_{out}/V_S [V/V]	*Q*	V_{out}/V_S [V/V]	*Q*
PISOT (N=3)	49.7883	47	19800	29	20400	**29**	12900
Single (N=1)	49.8486	**84**	84500	33	35700	28	30200

Future work:

- Understand *Q* decrease
- Model impact of load impedance & Q_{elec}

Models and Analysis

Single-substrate (N = 1) equivalent circuit:

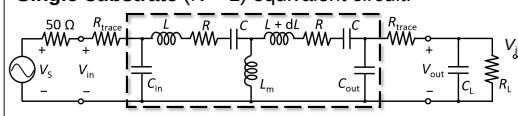

Stacked substrates:

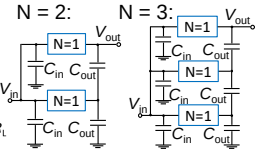

- Inter-resonator coupling modeled by L_m
- Asymmetric mass loading **d*L*** → Frequency difference **d*f***
- Voltage gain is a strong function of:
  df
  Load (R_L, C_L)
  Q

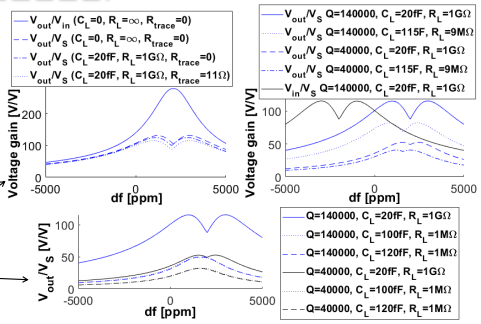

Accomplishments:

- **First demonstration of single-crystal AT-cut quartz as a two-port piezoelectric transformer**
  - **High *Q* & gain** advantageous for low-power radios
  - Enables impedance matching with readout circuit
  - Much **smaller form factor** than currently used in wake-up receivers
- Demonstrated passive open-circuit **voltage gains >2x higher than previous state-of-the-art** in two-port micromechanical PT
- Implemented compact RF front-end in an established, **commercially available process**
  - Facilitates transition into Army technology
- Demonstrated **17% increase in voltage gain using PISOT** techniques, i.e., "stacking" quartz substrates

Advanced Catalysts and Pyrolysis Process for Upgrading Biomass to Useful Chemicals/Fuels

Sampath Gunukula, Laleh Emdadi, Dat T. Tran
(FCDD-RLS-DE)

Project Goals

- Develop advanced catalysts and compact pyrolysis process to make value added chemicals/fuels from indigenous biomass to reduce Army energy logistic costs and to respond to the oil supply disruptions at the time of war

Specific Objectives

- Investigate the synthesis of in-situ hydrogen for the hydrodeoxygenation of pyrolysis oils
- Synthesize novel hydrodeoxygenation catalysts by incorporating Nickel to the 2D-lamellar zeolite
- Determine the optimal pyrolysis and hydrodeoxygenation process conditions (temperature and vapor residence time) to maximize oil yield as well as its quality
- Perform process simulations to determine the total size, weight, and efficiency of upgrading a low energy density biomass (woodchips/switchgrass) to a high energy density chemicals/fuels
- Study pyrolysis auger reactor for the biomass pyrolysis
- Investigate the mechanism to reduce coke formation on the catalyst surface during the hydrodeoxygenation process

Conceptual Process Design

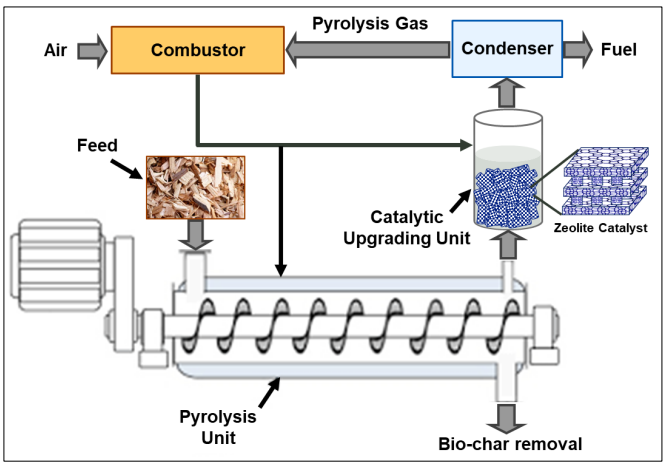

Novel Catalyst Development

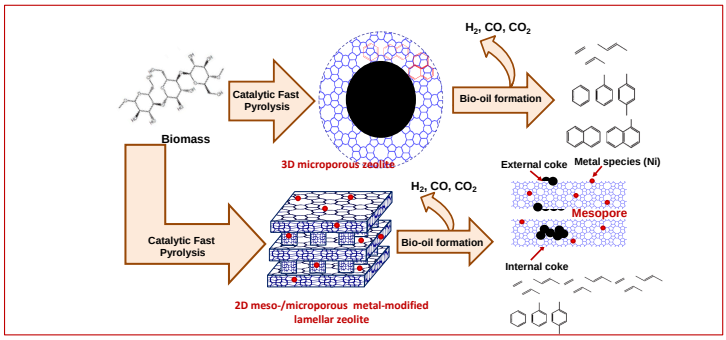

- Catalyst deactivation results from slow mass transport of bulky molecules into/out of zeolite structure and coke formation.
- Selectivity of the CFP reaction can be tuned by meso-/microporous structure of lamellar zeolite and change of its acidity by metal modification.
- Coke formation decreases due to the change in zeolite structure and acidity.
- Ni facilitates the production of H_2 from bio-oil compounds and decreases the need of ex-situ H_2 supply.

Process Modeling Methodology and Preliminary Size, Weight, and Efficiency Calculations

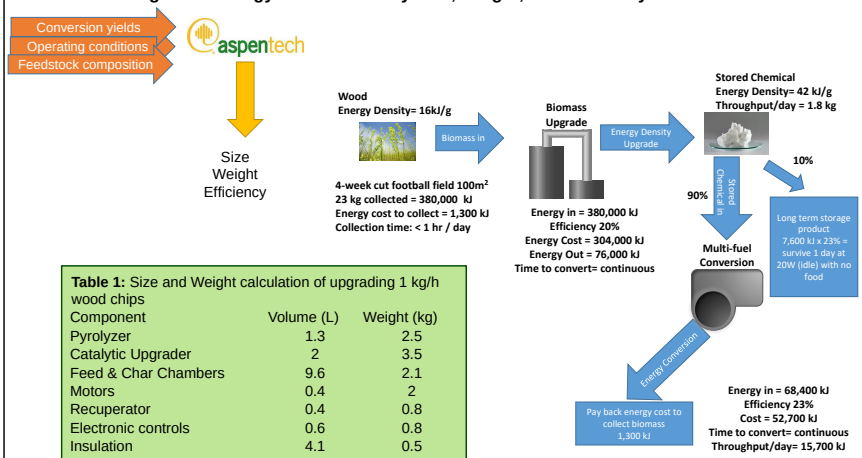

Table 1: Size and Weight calculation of upgrading 1 kg/h wood chips

Component	Volume (L)	Weight (kg)
Pyrolyzer	1.3	2.5
Catalytic Upgrader	2	3.5
Feed & Char Chambers	9.6	2.1
Motors	0.4	2
Recuperator	0.4	0.8
Electronic controls	0.6	0.8
Insulation	4.1	0.5
Separator	0.6	0.4
Fuel Tank	2.5	0.3
Transducers	0.2	0.3
Condenser	0.1	0.2
Catalytic Combustor	0.03	0.06
Free space	10.7	0
Total	**33**	**13**

The preliminary calculations show that the net energy of upgrading the wood chips to biofuel is positive. Additionally, the size and weight of compact pyrolysis process are found to be practical.

Catalyst Characterization

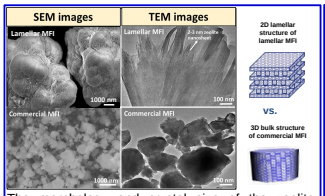

The morphology and crystal size of the zeolite particles were examined by SEM and TEM techniques.

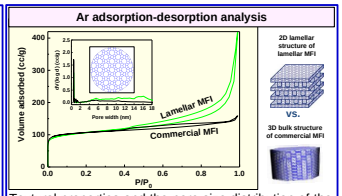

Textural properties and the pore size distribution of the zeolite catalyst were determined from the measured Ar isotherms.

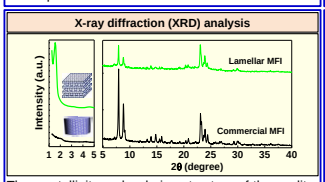

The crystallinity and ordering structure of the zeolite catalyst were determined by XRD measurements.

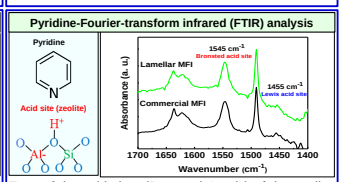

Type of the acid sites (Brønsted, Lewis) of the zeolite catalyst and their ratio were determined by pyridine-FTIR technique.

Evaluation of Pyrolysis Process Performance

- Measure the yields of pyrolysis oil, char, and gas
- Measure the water content of pyrolysis oil using the Karl Fischer Titration
- Perform the CHNO/S analysis of pyrolysis oils to determine the carbon, hydrogen, nitrogen, oxygen, and sulfur content of pyrolysis oils
- Perform GC-MS analysis to identify the pyrolysis oil compounds (acids, alcohols, aldehydes, sugars, and phenols)

Evaluation of Catalyst Performance

- Measure the mass and energy yields of upgraded pyrolysis oils
- Perform the CHNO/S analysis of upgraded oils to measure the quality
- Characterize the catalyst surface after upgrading pyrolysis vapors
- Perform catalyst on stream studies to determine the catalyst life
- Investigate the effectiveness of oxidation process as a method to regenerate catalyst

Findings/Outcomes

- A compact pyrolysis process to upgrade locally available biomass to a high energy density chemical/fuel for the Army purposes
- Understanding the mechanism to reduce coke formation on the catalyst surface without compromising oil yields and quality

Catalytic Oxidation of Propane over Palladium Alloyed with Gold: An Assessment of the Chemical and Intermediate Species

Haval Kareem and Dat T. Tran
CCDC Army Research Laboratory

ABSTRACT

The development of effective routes to clean energy production and air pollutant elimination is important for energy and environmental sustainability. Catalysis plays a central role in establishing such routes, but a major challenge is the design and preparation of active, robust and low-cost catalysts for the targeted catalytic reactions. Herein, this work reports a highly-effective thermochemical pathway for design, synthesis, and characterization of nanoalloy catalysts for propane oxidation. In particular, we focus on detecting and monitoring the nanoscale evolution of surface catalytic sites by probing the chemical and intermediate species on the catalysts in correlation with the bimetallic composition

Introduction[1-3]

- Emissions from vehicles and power station using liquefied petroleum gas (LPG) contribute to the main source of harmful volatile organic compounds (VOC)s
- Catalytic combustion is considered a more efficient way for CO, and propane removal compared to thermal decomposition
- Agglomeration of monometallic catalyst constitutes a major challenge
- Bimetallic catalysts are considered a promising alternative in terms of stability and high activity in comparison with monometallic
- The understanding of the surface catalytic sites is important for the design of the bimetallic nanoalloys catalysts

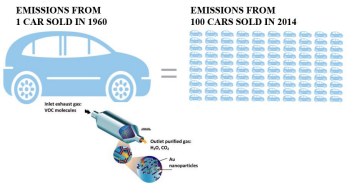

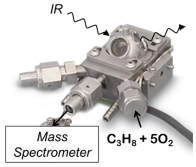

Nanoalloy

- Effect of surface energies of the component element
- Differences in atomic sizes
- Charge transfer between the different atomic species
- Strength of binding to surface ligands or support materials

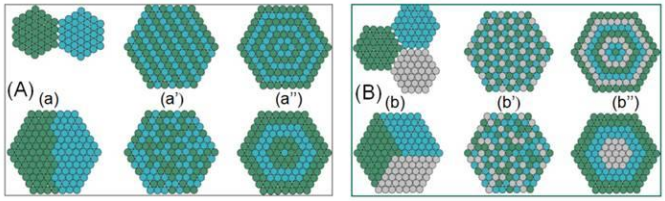

(a, b); ordered or random alloy structures (a', b'); and simple core-shell and multiple core-shell structures (a", b")

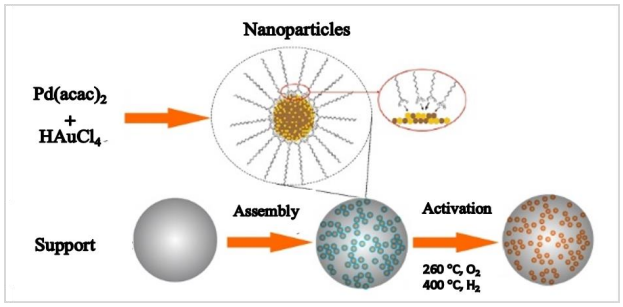

Morphology

➢ HAADF-STEM, EDS, TEM, and HRTEM

- Size of the nanoparticles 6.5 ±0.6 nm
- Good nano-crystallinity, surface segregation in $Pd_{91}Au_9$

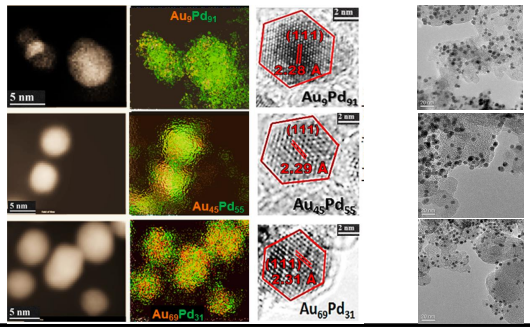

Catalytic Activity

- The measurement of the catalytic activity focused on PdAu NPs of different compositions supported on TiO_2 and Al_2O_3
- The catalytic activity depends on the bimetallic composition and the chemical nature of the support exhibiting the order of $Pd_{55}Au_{45}$ > $Pd_{91}Au_9$ > Pd_{31} Au_{69} for both TiO_2 and Al_2O_3 supported catalysts
- The PdAu/TiO_2 catalysts show higher activity than PdAu/Al_2O_3

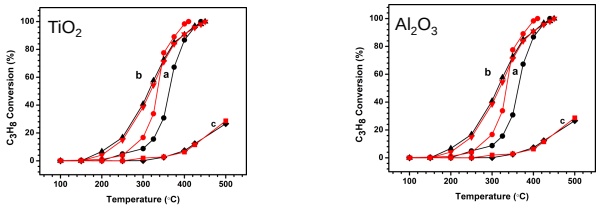

$Pd_{91}Au_9$ (a, circle); $Pd_{55}Au_{45}$ (b, triangle); and $Pd_{31}Au_{69}$ (c, square).

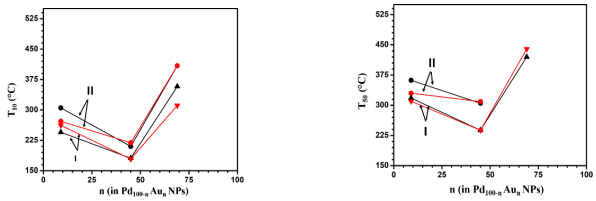

Characterization -DRIFT

- Evolution of oxy-carbon bands in the range of 1730-1330 cm^{-1}
- Intensity of intermediate species depends on NPs composition
- The intensities of the bands become stronger in case of Pd >50% alloys
- Formate and bicarbonate were detected on Pd-rich and Pd~50% alloys

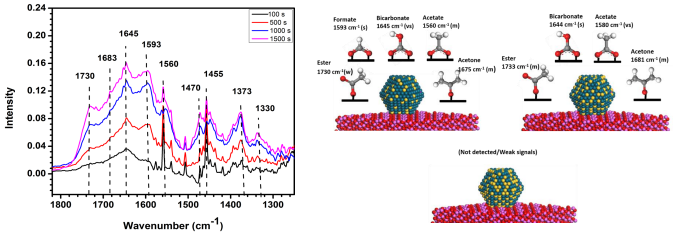

CONCLUSIONS

- Alloying Pd with Au in the catalyst with an optimal composition can enhance the catalytic activity for propane oxidation
- Strong composition dependence of the catalytic activity
- The results have revealed not only an activity maximum at Pd:Au ~50:50 ratio
- The absence of adsorbed formate and the reduced amount of adsorbed bicarbonate species Pd~50% PdAu alloy is linked to the higher activity in terms of achieving a complete C-C cleavage
- DFT calculations shows a maximum adsorption energy for propane over Pd:Au ~50:50

Path Forward/ Acknowledgement

- Investigations of nanoparticles, nanowire, nanotube catalysts in terms of size, shape, composition, and surface properties for gas phase reaction
- Comprehensive computational modeling to gain further insights into the structure-activity correlation

❑ We thank Dr. Derrick Mott, from JAIST for the help with morphology. Research was a joint collaboration work between Binghamton University and ARL

REFERENCES

1. M. Baldi, E. Finocchio and F. Milella, *Appl. Catal., B*, 1998, **16**, 43-51.
2. C.-H. Lai, C.-C. Chang, C.-H. Wang, M. Shao, Y. Zhang and J.-L. Wang, *Atmos. Environ.*, 2009, **43**, 1456-1463.
3. S. C. Kim and W. G. Shim, *Appl. Catal., B*, 2009, **92**, 429-436.

BEYOND VALIDATION ACCURACY: HOW TO DEVELOP A MACHINE LEARNING MODEL YOU CAN TRUST AND UNDERSTAND

John S. Hyatt[1,2] and Michael S. Lee[1]
[1]CCDC Army Research Laboratory, [2]Oak Ridge Associated Universities

ABSTRACT

Validation accuracy is a necessary *but not sufficient* criterion for evaluating a model's performance during training. A model with high validation accuracy during training may still be vulnerable to adversarial attacks, overconfident in its predictions of out-of-distribution data, or incomprehensible to a human. Such flaws have real-world consequences, but are still rarely addressed during model development. Using free, readily-available tools, we demonstrate that to train a classifier that is robust against these flaws, additional criteria besides validation accuracy are needed.

MOTIVATION[1-8]

Model design is HARD. Classifiers today optimize validation accuracy only, not:

- Ability to handle out-of-distribution data
- Explainability/trustworthiness
- Resistance to adversarial examples

LOOKING FOR A ROBUST CLASSIFIER

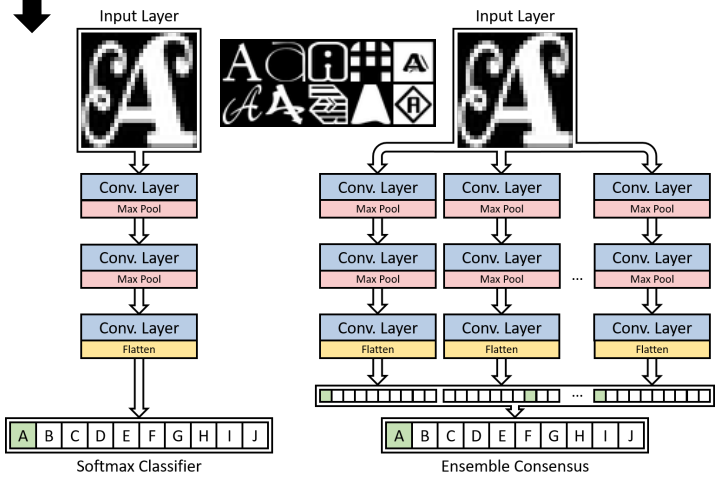

notMNIST dataset[10]:

- 28×28×1 images of letters A – J
- Wide variation within a class

Model candidates:

- **Components** (3-layer stacked convolutional neural networks)
- **Ensembles** (2, 3, 9, and 27 components, trained independently)
- **Grouped** (identical to ensembles, but not trained independently)
- **Wide** (identical to components, but 8× the kernels)

All have nearly identical validation accuracy (94.9±0.5%)

FEATURE VISUALIZATION (DEEP DREAMING)[11]

Generate images that maximize activation of 1 class.

- Do these resemble actual letters?
- Illegible except for grouped models, large ensembles

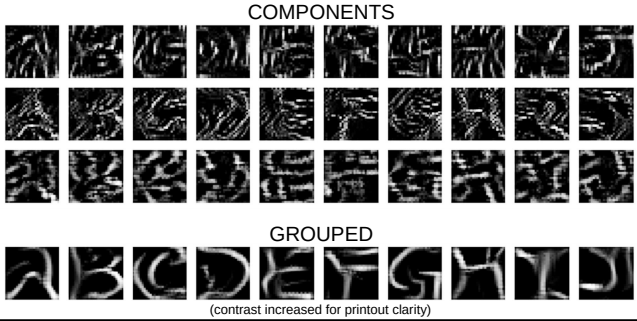

OUT-OF-DISTRIBUTION DATA[9]

Is model overconfident w.r.t. out-of-distribution predictions?

- Leave one class out of training
- Evaluate softmax predictions for that class's validation set
- Repeat for each class, comparing **in-** and **out-of-**distribution
- Plot ROC curve (function of discriminator threshold p_{thresh})
- Components, wide models, small ensembles all too overconfident

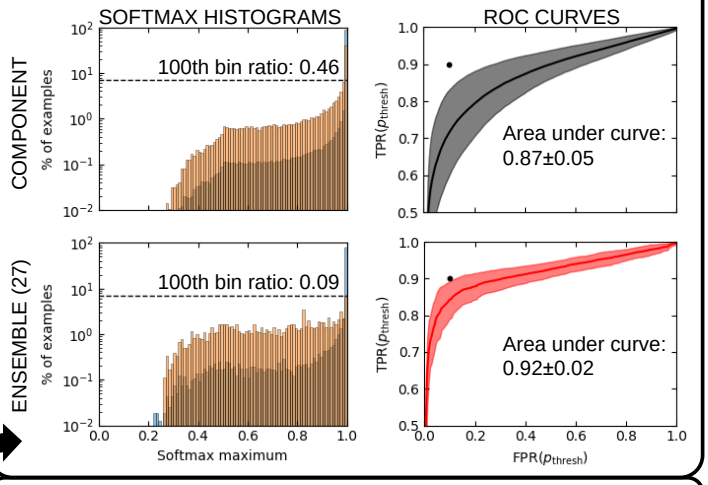

ADVERSARIAL EXAMPLES[12]

Small perturbation causes model to misclassify image.

- Generated w/ CleverHans library
- 3 attack methods: FGSM, MIM(∞-norm and 2-norm)
- Plot % misclassified vs. magnitude of perturbation
- Takes 2×–5× larger perturbations to fool grouped models and large ensembles (compared to components)

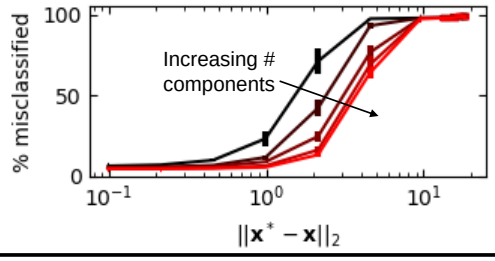

CONCLUSIONS

All models have same validation accuracy, but grouped models and large ensembles better in all other respects:

- Much less overconfident on out-of-distribution predictions
- Out-of-distribution data more easily identified w/ discriminator
- Produce legible dreamed images instead of noise
- Significantly more resistant to adversarial attacks

REFERENCES

[1] Barr, A., "Google Mistakenly Tags Black People as Gorillas, Showing Limits of Algorithms." *Wall Street Journal* (2015).
[2] Hunt, E., "Tay, Microsoft's AI chatbot, gets a crash course in racism from Twitter." *The Guardian* (2016).
[3] Angwin, J., Larson, J., Mattu, S., and Kirchner, L., "Machine Bias." *ProPublica* (2016)
[4] Thielman, S., "Facebook fires trending team, and algorithm without humans goes crazy." *The Guardian* (2016).
[5] Day, M., \How LinkedIn's search engine may reflect a gender bias." *Seattle Times* (2016).
[6] Garvie, C., Bedoya, A., and Frankle, J., "The Perpetual Line-Up." Georgetown Law Center on Privacy Technology (2016).
[7] Dodd, V., "UK police use of facial recognition technology a failure, says report." *The Guardian* (2018).
[8] Marshall, A. and Davies, A., "Uber's self-driving car saw the woman it killed, report says." *Wired* (2018).
[9] Hendrycks, D. and Gimpel, K., "A baseline for detecting misclassified and out-of-distribution examples in neural networks," in [*International Conference on Learning Representations*] (2017).
[10] Bulatov, Y., "notMNIST dataset." Machine Learning, etc., 08 September 2011 http://yaroslavvb.blogspot.com/2011/09/notmnist-dataset.html. (Accessed: 18 October 2018).
[11] Mordvintsev, A., Olah, C., and Tyka, M., "Inceptionism: Going Deeper into Neural Networks." Google AI Blog, 17 June 2015 https://ai.googleblog.com/2015/06/inceptionism-going-deeper-into-neural.html. (Accessed: 06 February 2019).
[12] Yuan, X., He, P., Zhu, Q., Bhat, R. R., and Li, X., "Adversarial examples: Attacks and defenses for deep learning," *CoRR* **abs/1712.07107** (2017).

ACKNOWLEDGMENTS

We thank Dr. Peng Wang and Dr. Manuel Vindiola for valuable discussions. Research was sponsored by the Army Research Laboratory.

Highly Reversible and Rechargeable Safe Zn Batteries Based on Concentrated Aqueous Electrolyte Systems

Lin Ma, Marshall Schroeder, Michael Ding, Oleg Borodin, Janet Ho and Kang Xu

FCDD-RLS-DC, Electrochemistry Branch, US Army Research Laboratory

Objectives

	Li	Zn
• Safety		
• Volumetric capacity[1]	2061 Ah/L	5855 Ah/L
• Volumetric energy density[1]	8244 Wh/L	23420 Wh/L

Same amount of energy, but ~1/3 volume with higher safety

Traditional Li-ion battery → *Unburden the warfighter* → Zn battery

- Develop novel concentrated aqueous electrolytes for next generation Zn batteries with improved performance to dramatically reduce the volume of deployed energy sources
- Unlock novel electrode/electrolyte chemistries to improve lifetime of Zn batteries for extended mission durations
- Expand temperature operation ranges of the electrolytes to accommodate Zn battery operation in all kinds of aggressive mission environment

Challenges

- Aqueous electrolytes struggle to reversibly cycle a Zn-metal anode[2]
- Oxidative stability of aqueous electrolytes limits available cathode options[3]
- Options of Zn salts for aqueous electrolyte are limited
- The purity of commercial $Zn(TFSI)_2$ salt is low

Approach

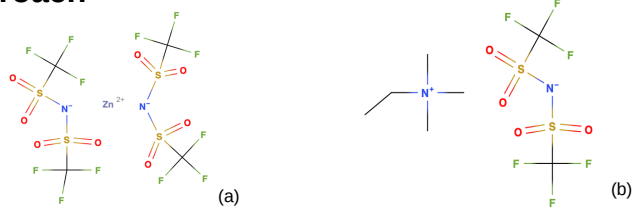

(a) (b)

Figure 1: chemical structures of synthesized salts in ARL: (a) $Zn(TFSI)_2$, (b) $Me_3EtNTFSI$.

$Zn(TFSI)_2$ synthesized in ARL has higher purity than commercialized ones, which meets electrolyte requirement well. $Zn(TFSI)_2$ containing electrolyte has higher conductivity than the state-of-art electrolyte (1m $LiPF_6$ in EC/EMC 3/7) in Li-ion cells.

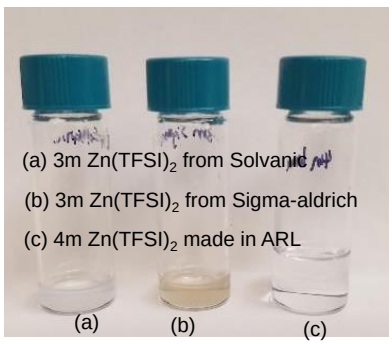

Figure 2: Comparison on aqueous $Zn(TFSI)_2$ solutions.

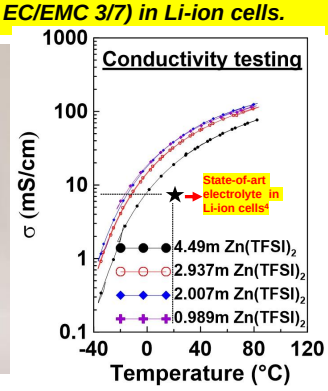

Figure 3: Conductivity testing on aqueous $Zn(TFSI)_2$ solution.

Results

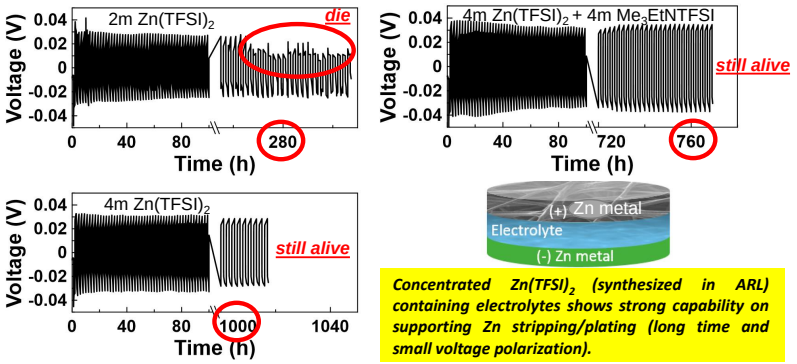

Concentrated $Zn(TFSI)_2$ (synthesized in ARL) containing electrolytes shows strong capability on supporting Zn stripping/plating (long time and small voltage polarization).

Figure 4: Zn/Zn cell cycling at room temperature with 0.5 mA/cm², 0.5 mAh/cm².

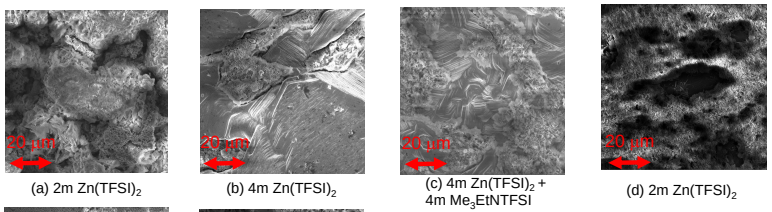

(a) 2m $Zn(TFSI)_2$ (b) 4m $Zn(TFSI)_2$ (c) 4m $Zn(TFSI)_2$ + 4m $Me_3EtNTFSI$ (d) 2m $Zn(TFSI)_2$

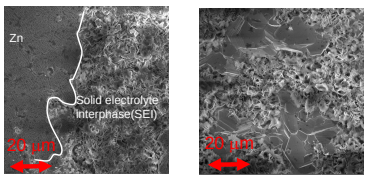

(e) 4m $Zn(TFSI)_2$ (f) 4m $Zn(TFSI)_2$ + 4m $Me_3EtNTFSI$

Figure 5: SEM images on Zn electrode after 200h cycling as shown in Figure 4 at fully discharged state with different electrolytes as labelled. Zn stripped side (a-c); Zn plated side (d-f).

Concentrated $Zn(TFSI)_2$ electrolytes made the surface more condensed and form more SEI species.

HNVO/Zn full cell cycling data @30°C showing substantial improvements in the ARL electrolyte systems over the commercial top-performing $ZnSO_4$ electrolyte.

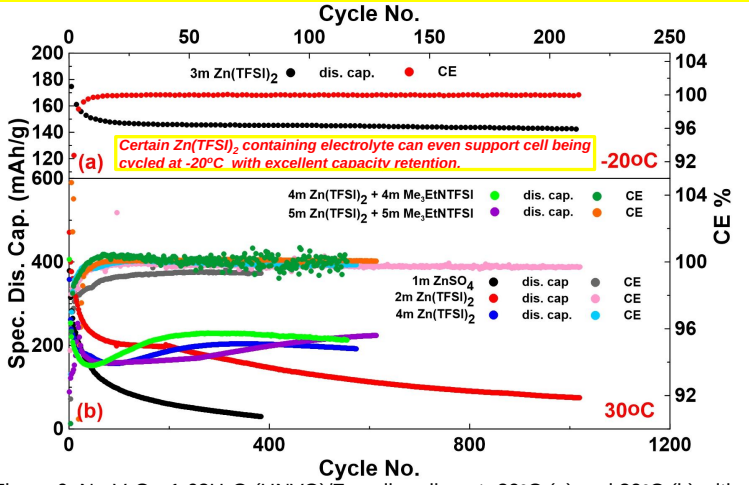

Figure 6: $Na_2V_6O_{16}{\cdot}1.63H_2O$ (HNVO)/Zn cell cycling at -20°C (a) and 30°C (b) with 300 mA/g.

Conclusions

Pure $Zn(TFSI)_2$ and $Me_3EtNTFSI$ salts were successfully synthesized in ARL. With the increase of $Zn(TFSI)_2$ concentration, the performance of Zn stripping/plating was dramatically improved. With the addition of $Me_3EtNTFSI$, HNVO/Zn cells show higher specific capacity and better capacity retention.

Path forward

Continued optimization, testing and characterization will lead to further IP and potential scale-up efforts with Industry/Academic collaborators.

References

1.Winter et al., *Chem. Rev.*, 118 (2018) 11433-11456
2.Li et al., *Nano Energy*, 62 (2019) 550-587
3.Pan et al., *Adv. Energy Mater.*, 8 (2018) 1800589
4.Logan et al., *J. Electrochem. Soc.*, 165 (2018) A21-A30

Acknowledgements

L.M. thanks JCESR and ORAU for funding. This research was conducted under the auspices of Army Research Laboratory under cooperative agreement number W911NF-19-2-0046.

Factors Effecting Metal Doping on Two-Dimensional and Three Dimensional Mordenite Framework Inverted (MFI) Zeolite for Chemical Energy Dense Production

Luther Mahoney, Ph.D.; Laleh Emdadi, Ph.D.; and Dat Tran, Ph.D.

Catalysis and Reaction Technology Team, Power Components Branch, Sensor Electron and Electronic Directorate, FCDD-RLS-DE CCDC Army Research Laboratory

Abstract

This research study delineated the effects of pore morphology and metal dopant in microporous and micro-mesoporous zeolite solid acid catalysts in converting ethylene to liquid aromatics. Our hypothesis included novel catalysts with particular metal dopants could increase liquid aromatic yield with a reduction in the amount of carbonaceous (coke) species within the solid acid catalyst. We further hypothesized that optimal loading of dopant could increase the liquid aromatic product yield from introduction of Lewis acid sites. The two-dimensional (2D) zeolite solid acid catalysts outperformed the three-dimensional (3D) zeolites in liquid aromatic yield and in the reduction in coke species. Moreover, the metal-doped zeolites in 2D and 3D with gallium (Ga) and zinc (Zn) at two weight percent loading produced larger liquid aromatic yield. The yield of liquid aromatics was up to 41% using 2D zeolite Zn-Lamellar-MFI. The conversion of ethylene to products was 97 to 99%. These results will be used in converting aqueous ethanol to aromatics, such as 20% (by volume) aqueous ethanol.

Background

Microporous zeolites are within a class materials denoted from their pore diameter depending the pore diameter with the International Union of Pure and Applied Chemistry (IUPAC) classification: (< 2 nm), microporous; (2-50 nm), mesoporous; and (> 50 nm), macroporous. Generally, the smaller the pore diameter leads to pore blockage with reduced mass-transfer and lower desired liquid aromatic products. Lower mass-transfer also potentially favors greater probability for producing carbonaceous undesired products.

Key variables that affect zeolite solid acid liquid aromatic yield included the following: (1) Si/Al ratio; (2) Bronston acid strength; (3) Lewis acid strength, dispersion, and loading; (4) textual properties including pore diameter, pore volume, and surface area; (5) dopant type and metal (dopant) loading; and (6) reaction variables like space velocity, pressure, and temperature.

The 3D zeolites have identical with regard to pore morphology. In contrast, 2D zeolites have different morphologies because of introduction of larger plane in one-direction. Likewise, the 2D zeolite acid sites vary because of there location be it on the surface or in the bulk. The 2D zeolites have greater surface area, which will affect the strength and concentration of acid sites. This surface vs. bulk porous phenomena is illustrated in the below graphical image.

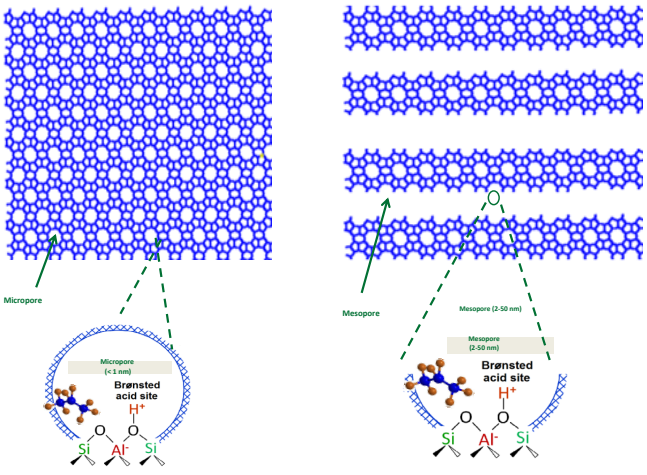

- **Low accessibility**
- **Low mass transport**
- **High accessibility**
- **High mass transport**

2D lamellar zeolites show higher activity & selectivity for ethene conversion to C_xH_y

Image Credit: Laleh Emdadi, Ph.D.

Experimental Setup

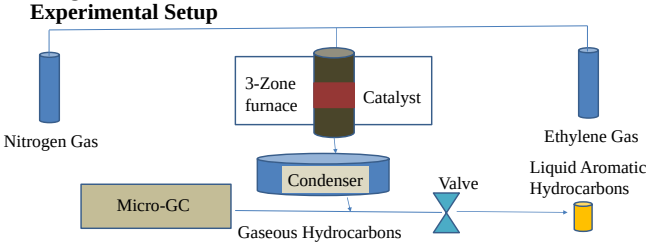

Characterization

The 2D and 3D zeolites were extensively characterized with high-angle annular dark-field-scanning transmission electron microscopy (HAADF-STEM) with energy dispersive X-ray spectroscopy (XRD), powder X-ray diffraction (XRD), argon physisorption, ultra-violet-visible (UV-Vis)-diffuse reflectance spectroscopy (DRS) spectroscopy, hydrogen (H_2)-temperature-programmed reduction (TPR), inductively coupled plasma-atomic emission spectroscopy (ICP-AES), Fourier transform-infrared (FT-IR) spectroscopy, ammonia-temperature programmed desorption (NH_3-TPD) and thermogravimetric analysis (TGA). In all of these characterization methods, the pore morphology was a major influence on the dopant location, dopant size, and dopant dispersion. Below is XRD, NH_3-TPD, and TGA of the six studied zeolite catalysts.

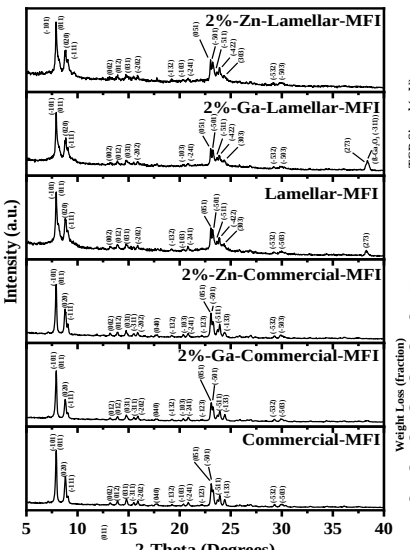

XRD

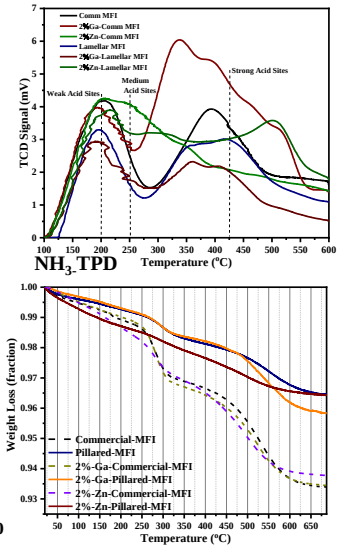

TGA

Results

Among the six zeolite catalysts evaluated, the 2%-Zn-Lamellar-MFI 2D zeolite had the largest liquid aromatic yield. The weight-hourly-space-velocity (WHSV) was shown to dramatically affect the liquid aromatic yield with lower WHSV leading to largest yield of liquid aromatics. TGA suggested that the pore morphology affected the type and amount of carbonaceous species formed. Low contact times lead to mainly gaseous products, and higher contact times produce greater amounts of liquid aromatic products. Overall, the pore morphology (2D vs. 3D) and dopant (Zn vs. Ga) had major influence on liquid product yield in addition to selectivity. Below is the gas-phase micro-GC analysis of 2%Zn-Lamellar-MFI zeolite on stream, and 8 h conversion.

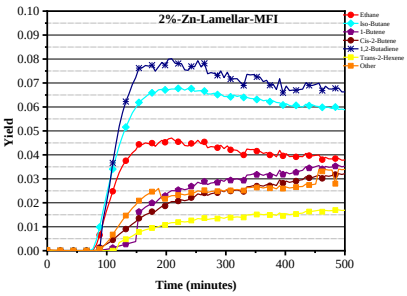

Gas-phase micro-GC analysis time on stream with 2%-Zn-Lamellar-MFI zeolite.

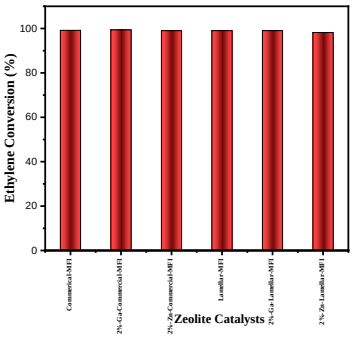

Ethylene conversion after 8 h for six zeolite catalysts evaluated.

Discussion/Path Forward

Scientific Questions answered: (1) Did the pore morphology affect the liquid aromatic yield, gas-phase yield, and coke deposition; what was the influence of metal dopant with regard to zeolite structure; does the reaction conditions influence the product yield and product selectivity; and does the zeolite structure doped amendable to aqueous ethanol to liquid hydrocarbon (ETH) reaction?

Next Step: Complete longevity studies with aqueous ethanol for ETH reaction.

Acknowledgements: Catalysis and Reaction Technology Team Colleagues, U.S. Army funding, and Oak Ridge Associated Universities (ORAU).

Reference: *Influences of metal-modification and lamellar zeolite structure on ethylene to liquid aromatics conversion reaction using MFI catalysts*, Luther Mahoney, Laleh Emdadi, Asher C. Leff, Dat T. Tran, Wei Wu, Sichao Cheng, Dongxia Lui, Chi K. Nguyen, Ivan C. Lee, *Fuel 256*, 115953:1-13 (10.1016/j.fuel.2019.115953), **2019**.

The Effects of Partner Knowledge in Virtual Reality

Shannon Moore & Michael Geuss

Background

- In Virtual Reality (VR), people may have little awareness of their partner:
  - Different physical locations
  - Unable to see one another
  - Unaware of the other's information, resources, and constraints
- A lack of familiarity with others' situational constraints can increase the likelihood of making dispositional attributions (Cramton, 2007).
- Greater familiarity with partners could help avoid negative attributions when teams underperform/disagree.
- Our own attitudes are functional (Katz, 1960). Thus, knowledge of others' attitudes should enable us to better anticipate others' behavior (Sanbonmatsu et al., 2011).

Hypotheses

Pairs who were familiar with each others' attitudes would be more accurate and faster and report better communication quality.

Attitude Familiarity will moderate negative effects of working in virtual reality.

Methodology

Player 1 vs. Player 2 View in VR

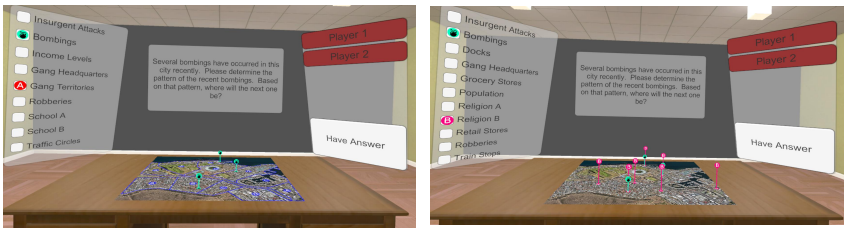

Desktop vs. VR Display

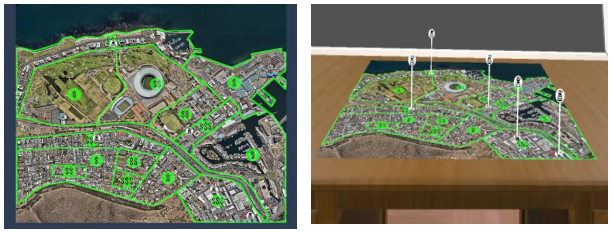

- Participants (23 pairs) viewed 4 maps (2 on desktop monitors, 2 in VR) where they had to identify information, determine patterns to events, and predict future events.
- Each partner had access to unique variables and consistent 'outcome' variables.
- Pairs were randomly assigned to either the Attitude Familiarity or Control condition.

Results

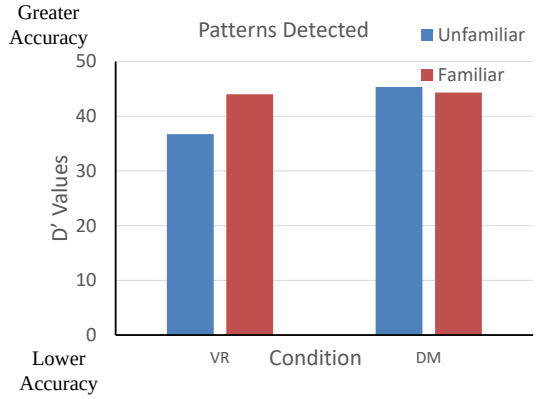

Result #1: Familiarity significantly improves accuracy at assessing patterns in VR and ability to predict future events overall. No effect for identifying information.

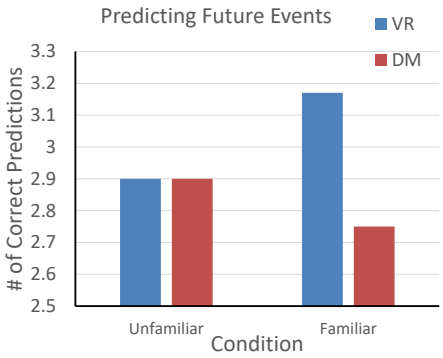

Result #2: Familiar pairs responded more quickly than unfamiliar pairs and even more so when that pair had prior experience with VR.

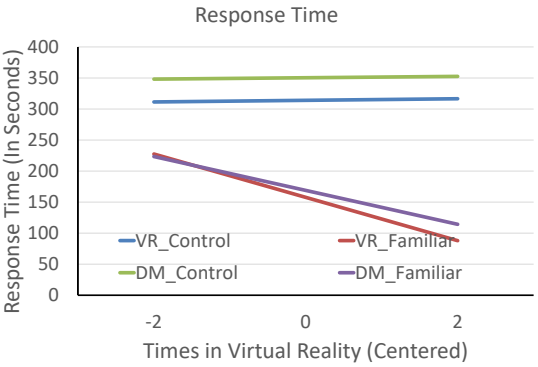

Result #3: Overall, pairs felt they communicated worse in VR.

Yet we know performance in VR overall did not suffer (Moore, Geuss, & Campanelli, 2019)

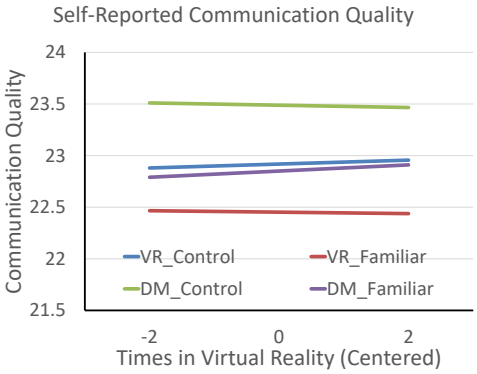

UNCLASSIFIED // APPROVED FOR PUBLIC RELEASE

Design, Synthesis, and Photophysical Investigation of Novel Iridium(III) Acetylacetonate Bisphenylquinoline Complexes

INTRODUCTION

Due to their tunable photoreactivity and light absorbing properties, organometallic iridium(III) complexes have a wide variety of applications such as phosphorescent dopants in organic light emitting diodes (OLEDs), chemical sensing, light harvesting for solar cells, and photodynamic therapy.[1]

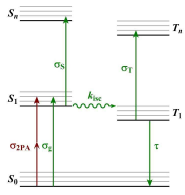

Particularly, our team is interested in their non-linear optical (NLO) properties such as reverse saturable absorption (RSA) and two-photon absorption (2PA).[2-4] The Jablonski diagram on the left illustrates the photophysical processes that our team studies related to 2PA and RSA.

OBJECTIVE

Design, synthesize, and characterize organometallic iridium(III) complexes containing phenylquinoline cyclometalating ligands in order to achieve panchromatic absorption in the ground state and excited state.

SYNTHESIS

Ligand Synthesis

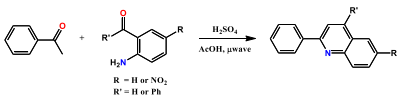

The ligands were synthesized via microwave-assisted Friedländer condensation of the appropriate amino-benzaldehyde or amino-benzophenone derivative with acetophenone according to modified reported procedures on the 0.5 gram scale.[5,6]

Complex Synthesis

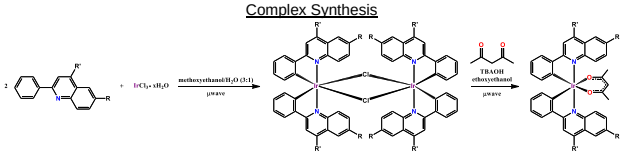

After successfully obtaining the ligand, the $[Ir(C^N)_2(\mu\text{-}Cl)]_2$ dimer was synthesized by mixing 2 equivalents of the ligand with $IrCl_3$ hydrate in a methoxyethanol/water (3:1) mixture and subjecting the reaction to microwave irradiation.[7] The target compounds were then synthesized by combining the $[Ir(C^N)_2(\mu\text{-}Cl)]_2$ dimer, acetylacetone (acac), and tetrabutylammonium hydroxide (TBAOH) in ethoxyethanol and subjecting the reaction to microwave irradiation. After purification via column chromatography, 4 complexes were obtained.

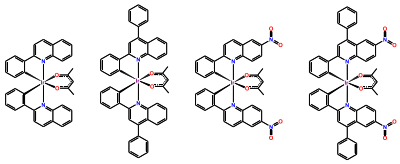

$[Ir(pq)_2(acac)]$ (1) | $[Ir(dpq)_2(acac)]$ (2) | $[Ir(NO_2pq)_2(acac)]$ (3) | $[Ir(NO_2dpq)_2(acac)]$ (4)

The complexes were characterized by ^1H NMR and single crystal x-ray crystallography confirming the structure to be the typical isomer for $[Ir(C^N)_2(acac)]$ of *cis-C,C/trans-N,N* geometry with typical bond lengths of Ir-C = 1.99 Å, Ir-N = 2.08 Å and Ir-O = 2.16 Å (data is an average of the four complexes).

Photophysical Characterization

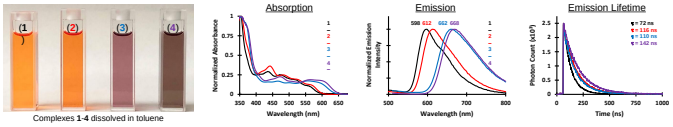

Complexes **1**-**4** dissolved in toluene

The absorption spectra of all four complexes were obtained in toluene. All samples exhibit the same characteristic absorption bands: ligand-centered (LC) π–π* transitions (300-400 nm) and metal-to-ligand charge transfer (MLCT) transitions (400-700 nm).[1] Also shown is the emission and emission lifetime data obtained in aerated toluene . All complexes are emissive when irradiated with 450 nm light with emission lifetimes ranging from 72 to 142 ns. As expected, the addition of the phenyl and/or nitro group resulted in a red shift of the absorption and emission. Unexpectedly, the emission lifetime increased with the addition of phenyl and/or nitro group counter to the energy gap law,[8] further experiments are needed to understand this trend. The addition of the nitro group results in a more dramatic red shift in the MLCT transition than the phenyl group, however, the phenyl group has a greater impact on the extending the lifetime of the excited state.

Transient Absorption

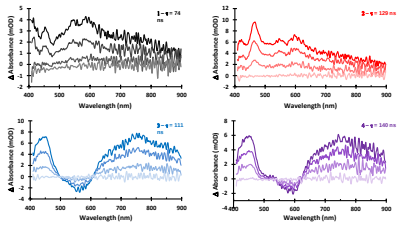

Transient absorption (TA) spectra were obtained in aerated toluene using pulsed 400 nm excitation (traces shown occur at 5, 50, 150, and 500 ns after the pulse). Complexes **1** and **2** exhibit broad excited state absorption. Whereas, complexes **3** and **4**, have bleaches ranging from ~500 nm to ~600 nm due to loss of the ground state absorption and little to no excited state absorption over this region.

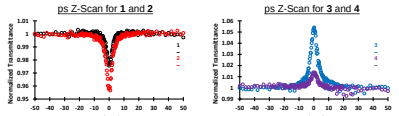

Open-aperture picosecond Z-scan experiments[9] of these complexes in aerated toluene were collected using 532 nm laser pulses (110 nJ, 30 ps FWHM). Complexes **1** and **2** exhibit RSA when irradiated with 532 nm, whereas complexes **3** and **4** show saturable absorption (SA) as expected based on the TA experiments.

Conclusions

Complexes **1** and **2** exhibit broadband RSA behavior, but lack broad absorption in the ground state. Complexes **3** and **4**, exhibit extended absorption in the ground state, but show SA behavior from 500 nm to 600 nm instead of RSA due to transient bleaches as seen in the TA spectra. Future work will be directed at designing and synthesizing complexes that display both panchromatic absorption in the ground state and panchromatic RSA.

References: [1] Y. You, W. Nam, *Chem. Soc. Rev.* 2012, **41**, 7061. [2] K-Y. Kim, *et. al., J. Phys. Chem. B.*, 2006, **110**, 17302. [3] W. M. Shensky, *et al., Appl. Opt.* 2017, **56**, B179. [4] P. Zhao, *et al.*, *J. Phys. Chem. C.* 2017, **121**, 23609. [5] A. K. Nedeltchev, *et. al., Tetrahedron*, 2010, **66**, 9319. [6] G. C. Muscia., *et al.,Bioorg. Med. Chem. Lett.*, 2014, **24**, 1545. [7] T. M. Monos, *et. al., J. Org. Chem.*, 2016, **81**, 6988. [8] J. V. Caspar, T. J. Meyer, *J. Phys. Chem.*, 1983, **87**, 952. [9] M. Sheik-Bahae, *et al., IEEE J. Quantum Electron*, 1990, **26**, 760.

Acknowledgments: The authors would like to thank Dr. Fu Chem and Dr. Yinde Wang of the UMD Analytical NMR Service Center for their assistance with NMR measurements.

UNCLASSIFIED // APPROVED FOR PUBLIC RELEASE

POINT OF CONTACT:
Thomas N. Rohrabaugh, Jr., Ph.D.
Thomas.n.rohrabaugh.civ@mail.mil
301.394.1720

Co-Authors: Ryan M. O'Donnell, Trenton R. Ensley, Michael J. Ferry, Peter Y. Zavalij (UMD), and William M Shensky III

Additive Manufacturing of Ceramics with Oriented Microstructures

Dr. Andrew Rosenberger*, Dr. Nicholas Ku+, Dr. Lionel Vargas-Gonzalez+

**Oak Ridge Associated Universities, ARL Ceramics and Transparent Materials Branch*
+ARL, Ceramics and Transparent Materials Branch

Background:

Toughness is an important material property that influences ballistic performance and multi-hit capabilities in ceramic armor. However, despite their excellent hardness and strength most ceramics possess an inherently low toughness.

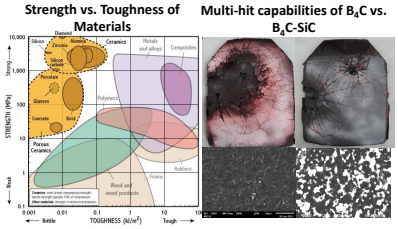

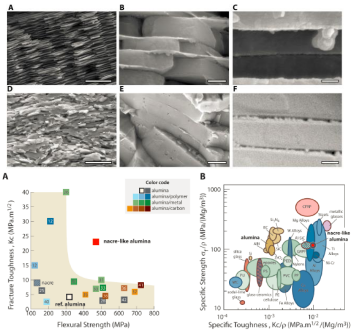

Bouville et al. "Strong tough and stiff bioinspired ceramics from brittle constituents, *Nature Materials*, 13, 508-514 (2014)

High toughness ceramics that maintain equivalent hardness and strength should be a breakthrough material enabling greater armor performance. Natural materials such as nacre, bone, or wood give blueprints for creating strong and tough materials through hierarchically oriented microstructures. Aligning fiber or platelet shaped grains within the microstructure can help create ceramic materials with both high toughness and strength.

Additive manufacturing inherently interacts with the printed material in a discrete, controllable manner, presenting a unique opportunity to control both shape and microstructure in a single, efficient process!

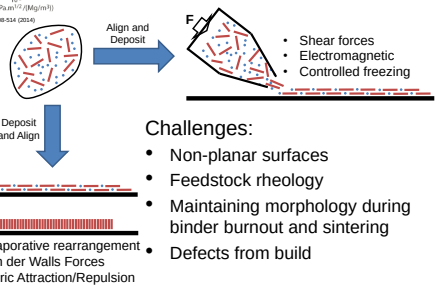

- Shear forces
- Electromagnetic
- Controlled freezing

- Evaporative rearrangement
- Van der Walls Forces
- Steric Attraction/Repulsion

Challenges:

- Non-planar surfaces
- Feedstock rheology
- Maintaining morphology during binder burnout and sintering
- Defects from build

Goal: *Develop Additive Manufacturing techniques to print ceramic parts with controlled, high-toughness bioinspired microstructures.*
Strategy: *Use pre-existing materials and methods; Al_2O_3, tape casting, to speed development and prove feasibility of concept*

Experimental:

Feedstock Development:

- Feedstock was created using stock materials and mixing process developed for direct ink writing methods at ARL
- Viscosity curves were obtained with parallel plate rheometer at different solids and platelet loadings

A16 Al_2O_3 Powder

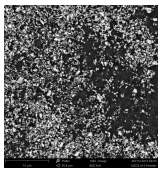

- α-Al_2O_3
- D_{50} = 0.4μm

Alusion Al_2O_3 Platelets

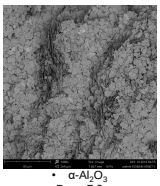

- α-Al_2O_3
- D_{50} = 7.9μm
- Thickness = 0.2μm

Tethon Genesis Photocurable Resin

- Acrylate based resin
- P = 1.07g/cm³
- Cures in UV-A light

Flaktek Speedmixer

- 800-2000RPM ramp
- Al_2O_3 media to break up agglomerates

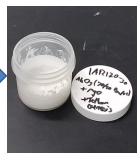

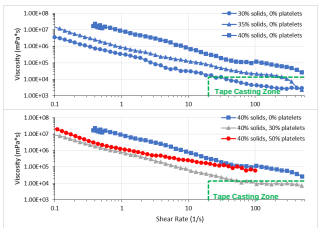

- Shear thinning behavior was observed in all compositions
- Platelet fraction had non-linear effects on viscosity
- Acceptable tapes were cast at viscosities up to 1000mPa*s

Tape Casting

- Materials were tape cast at 100mm/s with a 0.2mm gap
- Curing was done with a 400W UV lamp at 10s exposure time
- Good platelet alignment observed with SEM
- 3D printing was simulated by tape casting multiple 0.2mm layers up to a thickness of 5mm
- Specimens were cut out for sintering
- Max solids loading of 40vol% obtained

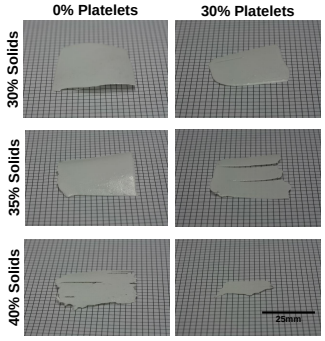

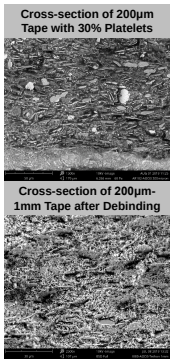

Sintering Cycle

- Debinding cycle of 10ºC/hr to 600ºC removed photopolymer without warping or cracking
- Due to low solids loadings, both cold isostatic pressing (CIP) followed by pressureless sintering and hot pressing were explored. 1wt% MgO was added as a sintering aid to all slurries

Pressureless Sintering

- CIP to ~55% theoretical density
- Various sintering cycles attempted; 2-stage 1600ºC/1500ºC-1Hr gave best results
- All had difficulty reaching full densification while limiting grain growth

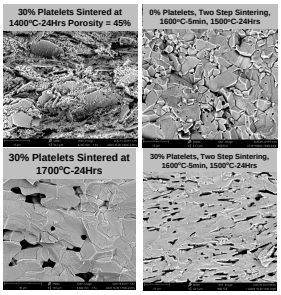

Hot Pressing

- Better able to maintain platelet structure while obtaining densification
- Good results obtained at a 15 min soak at 1275ºC with 65MPa pressure

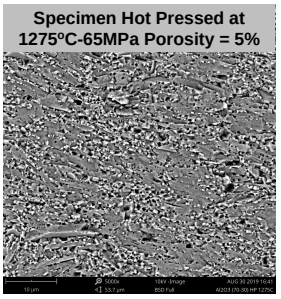

Mechanical Testing

- Vickers indentation tests were performed parallel and perpendicular to the texture orientation to qualitatively compare the effect of the anisotropic microstructure on toughness
- Porosity and grain pullout during polishing interfered with the resolution of the test, but the average crack length was shorter perpendicular to the platelets, indicating greater toughness
- Transgranular crack deflection around platelets was observed

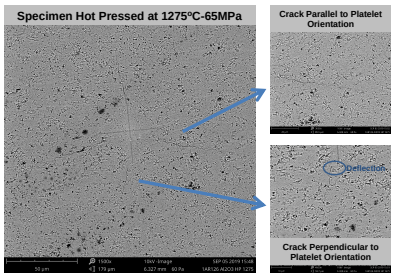

Conclusions & Future Work:

Potential route for producing high-toughness ceramics through AM has been demonstrated!

Feedstock:
- Further explore effects of powder size distribution and environmental conditions on viscosity
- Improve solids loading to 50%

Sintering:
- Explore sintering aids to enable pressureless sintering to full density
- Further develop hot pressing technique to eliminate porosity

3D Printing:
- Demonstrate process on Admaflex printer
- Adapt to armor materials (B_4C, SiC)
- Explore Direct-ink writing technologies for fiber alignment

Testing
- Quantitative mechanical and microstructure characterization
- Ballistic characterization

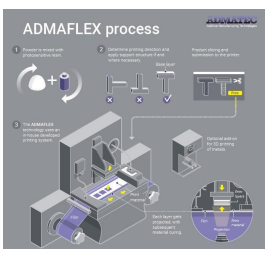

IoT in Smart Cities: Information Theoretic and Deep Learning Approaches to Improve Parking Solutions

Objectives

- To develop a model for overcoming limitations of existing machine/deep learning methods in order to predict the parking availability in IoT environment for smart cities when faced with data nuances, noise and nonlinearity challenges.
  - Impetus behind this work stemmed from Army's existing challenge to carry out its Multi Domain Operations (MDO) effectively.
  - Because military bases share many of the same characteristics as small cities, depend on many common electronic architectures and devices used in civilian environment, and the IoT gaining more traction, this concept can be applied to military installations.
  - The modernized smart bases improve parking, logistics, reduce costs, and help military staffers make better decisions in daily C2 (command and control) routine.

Approach

We prepare a dataset using the semantic vectors as input training, and the accuracy as the output target. We

1. **Perform a comparative analysis of our optimization approach to improve *k*-**

Step0: Given data, $X = \{x_i\}_{i=1}^n$, define $L^2 = \|x_i - x_j\| = \sqrt{\sum_l^n (x_{i,l} - x_{j,l})^2}$

Step1: Modify L^2 to $L_W^2 = \sqrt{\sum_l^n (x_{i,l} - x_{j,l})^2}$ for transformation parameter $W = \{w_i\}_{i=1}^n$, responsible for improvement in $k - Means$.
Step2: Measure this improvement by $Davies - Bouldin\ Index\ (DBI)$.
Step3: Define unconstrained optimization problem as $\min_W f(X, W)$
Step4: Find suitable W, by solving optimization problem in Step3.

2. **Classify the target accuracies using the family of *Chisini-Jensen-Shannon divergences (CJSDs)* based kernels in *SVM* classification.**

For probability distributions, $P = \{p_i\}_{i=1}^N$ and Q= $\{q_i\}_{i=1}^N$, family of $CJSDs$ is define as: $CJSD(P||Q) = \frac{1}{2}\left[\sum_{i=1}^N p_i log \frac{p_i}{M_i} + \sum_{i=1}^N q_i log \frac{q_i}{M_i}\right]$; where, M is a Chisini Mean. Its ***metric*** version is $M\text{-}CJSD(P||Q) = \sqrt{CJSD(P||Q)}$

Family of CJSD based kernel versions (Amplified & Scaled):

Amplified: $CJSD(P||Q)e^{-\frac{|x_i - x_j|^2}{2\sigma^2}}$; **Scaled:** $e^{-CJSD(P||Q)\frac{|x_i - x_j|^2}{2\sigma^2}}$

3. **Build a multi-layered *deep neural network (DNN)* for performance benchmark.**

Results

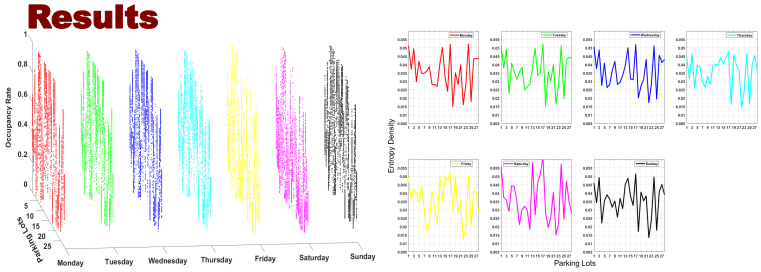

Figure. **(Left)** Similarity in occupancy rate on weekdays making data class discrimination a challenging task. **(Right)** Entropy Density clearly discriminates weekdays despite similarity in their patterns. For example, Saturday patterns (magenta) are relatively distinguishable from other weekdays identifying it as the busiest day of the week.

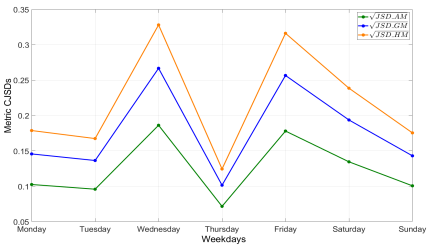

Figure. $M - CJSD$ provide higher separability between the probability distributions of each weekday and rest of the week in order:

$$\sqrt{JSD_{AM}} < \sqrt{JSD_{GM}} < \sqrt{JSD_{HM}}$$

Lower M-CJSD output implies more similarity between Thursday and remaining week. Higher $M - CJSD$ output for Wednesday and Friday implies less similarity.

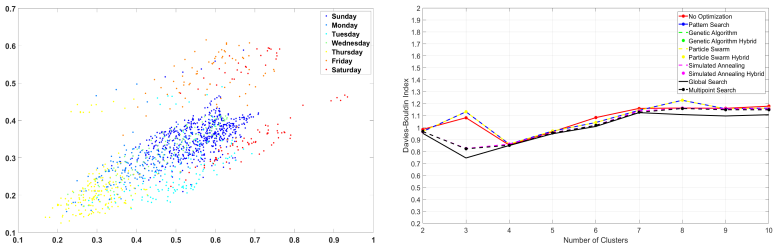

Figure. **(Left)** Optimal number of clusters found by GM distribution clustering. **(Right)** Smaller $Davies - Bouldin\ Index\ (DBI)$ value indicates that Multipoint Search (black line) performs better than all tested optimization methods, including when no optimization (i.e., no L^2 transformation) was performed (red line), transformed $k - Means$ is unable to find all 7 clusters corresponding to weekdays due to high class similarity.

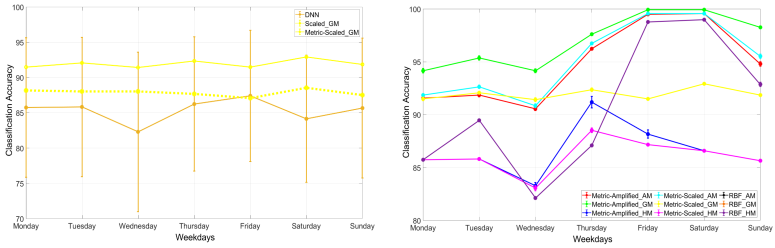

Figure. **(Left)** Error bars for $M - CJSD$ based and RBF kernels. Results are reported for 3 randomized data versions (AM, GM, HM). Notice that $Metric - Ampified_GM$ version (green) outperforms all other kernels achieving around 97% average accuracy, while RBF performs the same for each randomized data version (overlapping black, orange and purple lines with purple on top) achieving around 90% average accuracy. **(Right)** Error bars indicate that DNN achieves around 85% average accuracy with high standard error, while both $Scaled_GM$ and $Metric - Scaled_GM$ versions outperform DNN achieving around 88% and 92% average accuracy respectively. This result also shows a relative improvement in $M - CJSD$ over CJSD for $Scaled_GM$ version.

Path Forward

1. We will extend our analysis to a heterogeneous IoT environment on a big data, and consider the impact of IoT topology, connectivity, security, etc. on model performance.

2. We will focus on time series analysis to predict parking availability in densely populated smart city areas.

Conclusions

1. Modified *CJSDs* to *Metric-Chisini-Jensen-Shannon divergences (M-CJSDs)* satisfying *metric space* properties.

2. Introduced a family of new M-CJSD based kernels, namely, *Amplified, Scaled, Amplified-Scaled*.

3. Proved a number of mathematical properties for M-CJSDs, most importantly, their relationship to CJSDs, and validated them empirically.

4. Developed an information theoretic method for the measurement of car occupancy rates at parking lots during the weekdays.

5. Investigated a number of clustering algorithms, e.g., *GM distribution*.

6. Developed an optimization approach to modify k-Means clustering by transforming L^2-distances between data points.

Publications

1. P. K. Sharma and A. Raglin, "IoT: Smart City Parking Solutions with Metric-Chisini-Jensen-Shannon Divergence based Kernels," in Proceeding of 2019 IEEE Military Communications Conference (MILCOM-2019) [Under Review].

2. P. K. Sharma and A. Raglin, "IoT in smart cities: Exploring information theoretic and deep learning models to improve parking solutions," in The 5th IEEE International Conference on Internet of People (IoP-2019).

3. P. K. Sharma and G. Holness, "L2-norm transformation for improving k-means clustering," International Journal of Data Science and Analytics, vol. 3, no. 4, pp. 247–266, 2017.

4. D. H. Stolfi, E. Alba, and X. Yao, "Predicting car park occupancy rates in smart cities," in International Conference on Smart Cities. Springer, 2017, pp. 107–117.

POINT OF CONTACT: Piyush Sharma, Ph.D. (piyush.k.sharma.ctr@mail.mil, 301-394-5609)

Reconfigurable Properties in Layered Superstructures

Sina Najmaei[1], Chinedu. E. Ekuma[2], Adam. A. Wilson[1], Madan Dubey[1]
[1]Sensors and Electron Devices Directorate, United States Army Research Laboratory, Adelphi, MD 20783
[2]Department of Physics, Lehigh University, Bethlehem, PA 18015

Abstract: Reconfigurability is a highly desired material property and essential to enabling neuromorphic and quantum computing applications. 2D van der Walls layers are a unique set of materials with a distinctive structural opportunity to enable heterogeneous device concepts. Here we present a highly versatile and effective approach to reconfigure the electron and phonon behavior in 2D hafnium disulfide, through intercalation of organometallic sandwich compounds. Through controlled device structures we demonstrate a dynamic control of the cross-plane thermal and electrical conductivity of the devices by a factor of 4x and 1000x, respectively. Our findings unveils a comprehensive approach to tailor and design 2D materials properties for applications in high performance electronic and phononic devices.

Methods: We prepare the intercalated samples by exposing the host HfS_2 at elevated temperatures to the cobaltocene and chromocene dissolved in toluene. These experiments were done under environmental control inside a glovebox with oxygen and water vapor concentration less than 20 ppm and less than 0.05%, respectively.

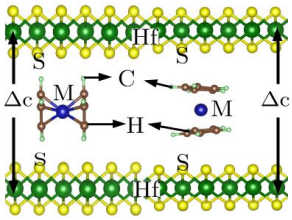

Material Characterization: We resolve two pair of peaks, related to the intercalated and un-intercalated regions, made of $4f_{7/2}$ and $4f_{5/2}$ orbitals separated by ~1.6 eV. The shift in the Hf peaks in the intercalated regions is indicative of charge transfer to the HfS_2 in both types of metallocenes. The valance band edge analysis shows a large shift in both intercalated samples towards negative binding energies that is indicative of charge transfer to the HfS_2 and a hift in the Ferr i levels of the ı aterials.

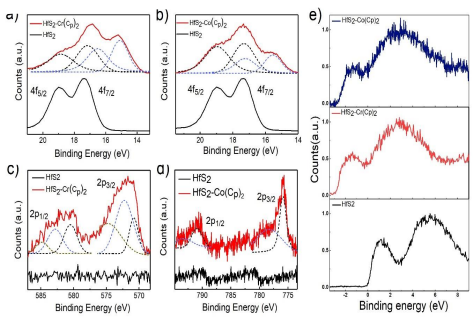

Theory: We perform first-principles spin-polarized calculations with the HSE06 hybrid functionals. The results show changes and a narrowing of the bandgap by ~0.80 eV while new states emerge below the conduction band edge relative to pristine HfS_2

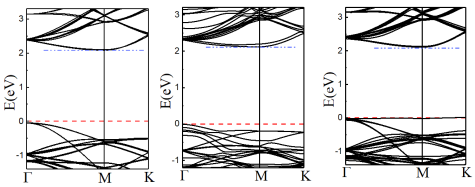

HfS_2 $HfS_2/Co(C_p)_2$ $HfS_2/Cr(C_p)_2$

Reconfigurability of Phonons: The measured Raman spectra shows the two prominent *Eg*(263.7 cm^{-1}) and *A1g*(338.0 cm^{-1}). The Raman spectra of the intercalated samples gives rise to a new peak and changes in the peak positions and linewidths relative to the reference sample.

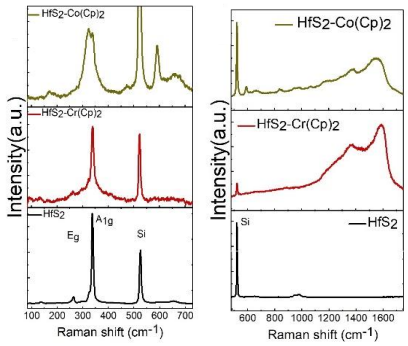

Phonon Dispersions: We compute the planar phonon dispersions and density of states for the pristine bilayer and the intercalated bi-layered HfS_2. Just as in the electronic spectra, the phonon spectra of HfS_2-$Cr(Cp)_2$ and HfS_2-$Co(Cp)_2$ share many commonalities. The calculations can be used to better understand the anharmonic effects in HfS_2 and its intercalated samples and provides a basis for understanding the temperature-endence of the Ram spectra.

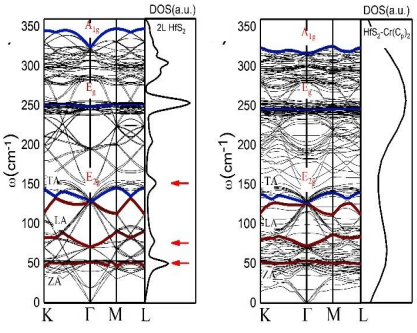

Reconfigurability in Phonon Anharmonicity: The temperature dependence of the Raman modes can inform us of the phonon decay mechanisms. It is clear that the complex interfaces in the intercalated samples facilitates many additional decay channels for optical phonons in HfS_2. after the intercalation of metallocenes it appears that the decoupling of the layers and mitigation of interlayer interactions

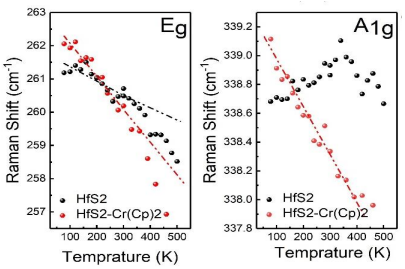

Reconfigurable Thermal and Electrical Properties: We perform time-domain thermoreflectance (TDTR) measurements and measure cross-plane thermal conductivity of roughly 0.34 $Wm^{-1}K^{-1}$ for HfS_2 and 1.45 $Wm^{-1}K^{-1}$ for HfS_2-$Cr(Cp)_2$ (a factor of 4 increase in thermal conductivity). We measure an in-plane electrical conductivity of 1.2×10^{-8}(S/μm) and this is increased by more than an order of magnitude to 1.5×10^{-7}(S/μm) and 2.45×10^{-7}(S/μm) for HfS_2-$Cr(Cp)_2$ and HfS_2-$Co(Cp)_2$ samples, respectively. This is attributed to the charge transfer from the intercalants to HfS_2. A decrease in the anisotropy ratios (σ_c/σ_a) for the cross-plane versus basal plane conductivity of electronic conductivities by a factor of ~ 6-20 is a result of a combined effect of material doping, and the increase in tunneling barrier height.

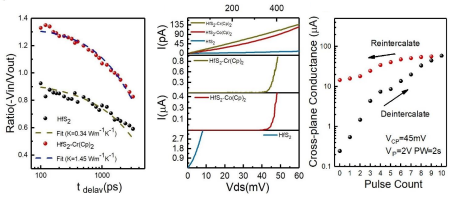

Conclusions: We have demonstrated a useful approach to dynamically reconfigure the electronic and phonon properties of layered materials through stacking of organic/inorganic materials.

References:

Najmaei, S; Peng, J; Chung, P; Dubey, M. Anharmonic Vibrational properties of Hafnium Disulfide Thin Films. in preparation

Najmaei, S; Peng, J; Chung, P; Dubey, M. Zone-center Phonons and the Role of Disorder on Vibrational Properties of Hafnium Disulfide Thin Films. *Applied Physical Letters* (2019)

Peng, J; **Najmaei, S**; Dubey, M; Chung, P. Structural, Phonon, and thermal properties of HfS_2: A first principles study. *Journal of Applied Physics* (2019)

Acoustic Wireless Power Transfer

Victor F.-G. Tseng, T. E. Drummond, S. S. Bedair, N. Lazarus
Sensors and Electron Devices Directorate, E&P Division, Power Components Branch

Overview

Acoustic (ultrasonic) WPT:
- **Higher efficiency than inductive WPT at larger distances**
- **Can transfer through air and metal**
- Smaller transducers, lower frequencies

Army relevance:
- Efficient on-soldier power distribution
  - Reduce batteries & cognitive burden
- Soldier power off-loading platform
- Eliminate bulky cables, enhance reliability

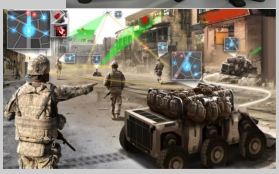

Photo courtesy of CERDEC

Wireless Power Technology Comparison

Through-air WPT distance comparison:

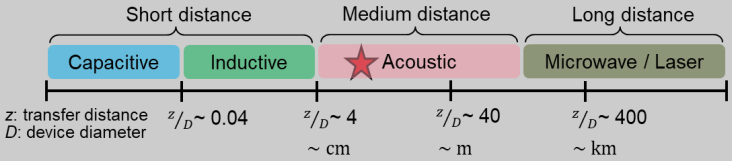

Through-metal WPT comparison:

- Acoustic waves can transfer through metal
- EM waves blocked by shielding

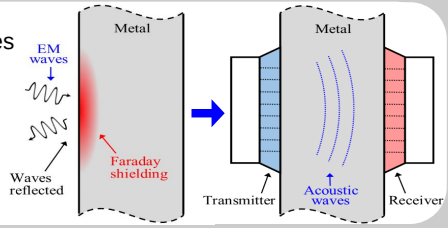

Through-air Acoustic Wireless Power

First demonstration of Phased Array Focusing:
- Electronically steer power beam to receiver location
- Acoustic focusing used to increase efficiency
- Power only transferred to focal point location

Acoustic WPT system:

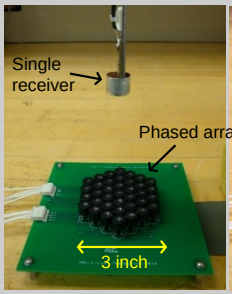

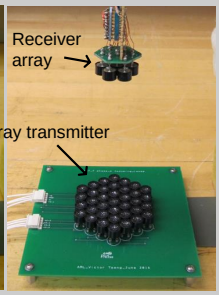

Acoustic modeling:

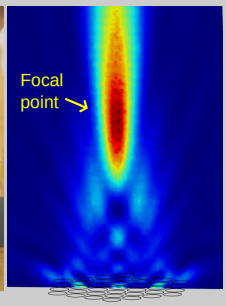

Results: Acoustic WPT vs Inductive WPT
- Verified that acoustic WPT is better at larger distance
- 2.6 times increase in efficiency using acoustic focusing
- 3.8 times increase in efficiency using receiver array
  - Power combining from receiver array is critical

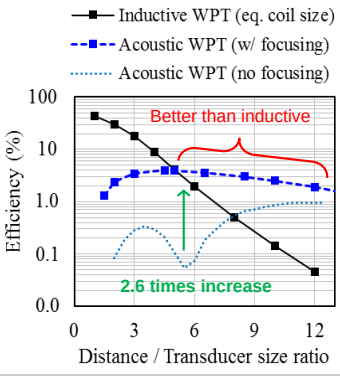

With receiver array:

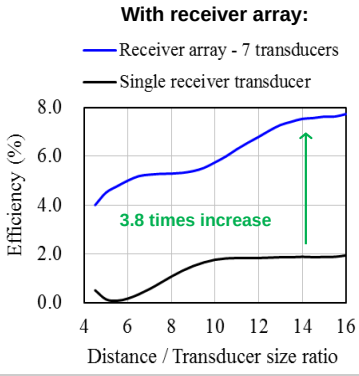

Future work:
- Improve focusing with miniaturized transducer design
- Improve acoustic impedance matching
  - Target efficiency: ~15% by 2020, ~20% by 2023
- Actively locate receiver position for power beaming

Transducer design:

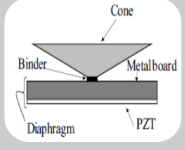

Receiver requests power: Transmitter beams power:

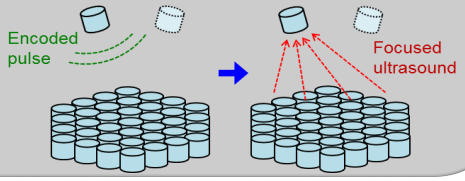

Through-metal Power & Data Transfer

Self-contained Sensor Node Embedded in Metal:
- Custom designed sensor node fully embedded in metal
  - For vehicle structural health monitoring
- Acoustic waves for power & data transfer
  - Power transfer to node (to charge battery)
  - Node responds with sensor data

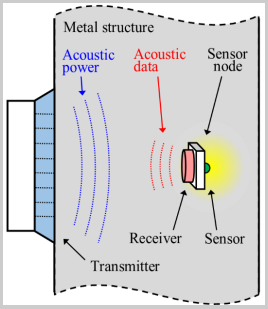

Sensor node sealed in fusible alloy:

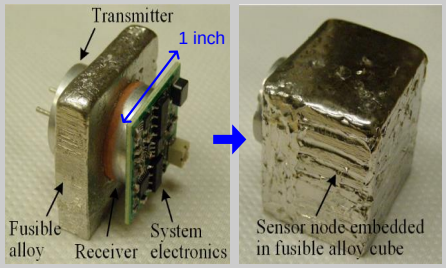

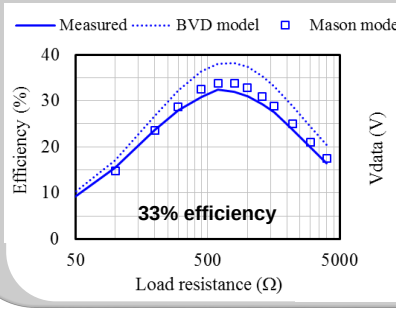

Back transmitted data:

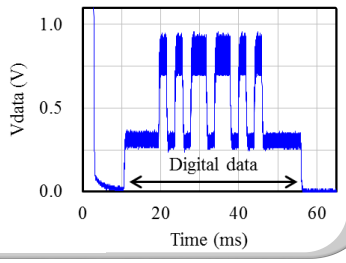

Lamb (Plate) Wave Power Transfer

Plate waves propagating in metal plates / tubes:
- Achieve longer distance WPT due to 2D confined waves
- Affected by standing wave modes of metal structure

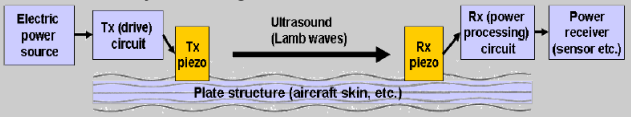

45-56% efficiency at 40 cm distance

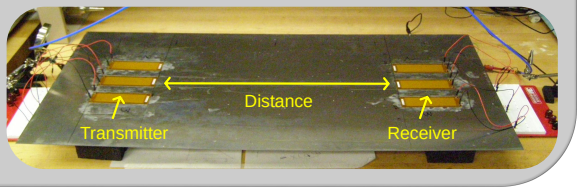

Tunable and tailorable thermal properties of solid-state materials

Adam A. Wilson, FCDD-RLS-DE, adam.a.wilson6.civ@mail.mil
Darin Sharar, Asher Leff, Jacob Wright, Jack Brody; FCDD-RLS-DE
Sina Najmaei, FCDD-RLS-RL; Chinedu Ekuma, Leheigh University

We seek to find materials with **dramatic change in thermal conductance:** over a **narrow operating temperature range**, or in response to **external stimulus**

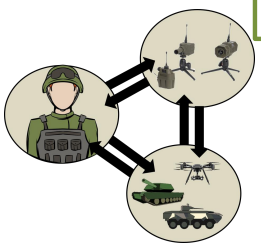

Novel (heat-based) methods for computing, communicating, disguising, identifying and decoying

Pulsed power thermal mitigation for directed energy combat systems

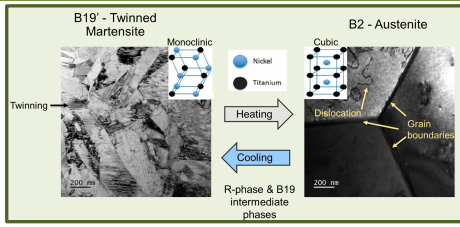

- Reversibly change grain-boundary density via Martensitic twinning
- Tailor and tune cubic phase properties by solution anneal and heat treatment.
- Thermal conductivity, latent heat tunable by processing conditions

This work

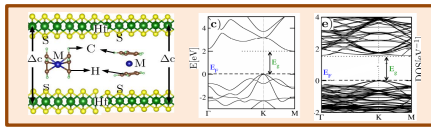

- Manipulate interaction between layers in van der Waals materials
- Intercalate and de-intercalate to change band gap properties (leads to **4x change in thermal conductivity**)

Tunable thermal materials are highly relevant to future Army needs

Current ARL efforts: Martensitic transformations and intercalation of layered materials

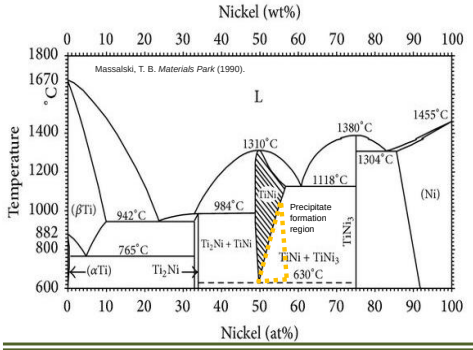

- Heat treatment and solution anneal allow us to tune precipitate formation and grain growth
- This affects:
  - defect density,
  - latent heat,
  - thermal conductivity
  - Transformation temperature

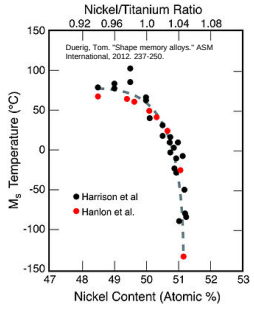

- Ni-rich materials drastically reduce transformation temperature
- Target precipitates remove Ni, which increases transformation temperature (confirmed through DSC, TEM & EDS)

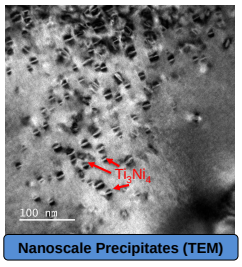

Nanoscale Precipitates (TEM)

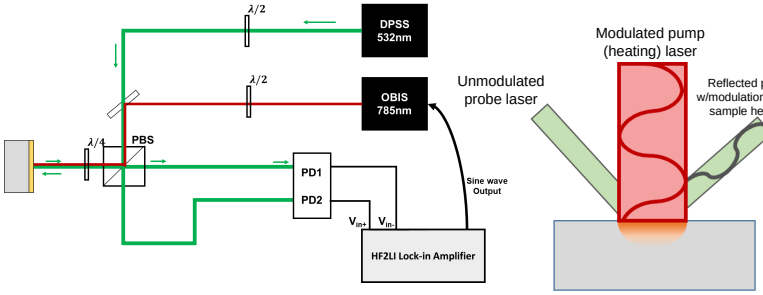

Frequency-domain thermoreflectance (FDTR) – a non-contact tool for exploring thermal properties with microscale resolution

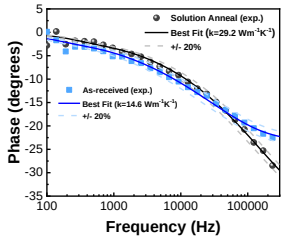

Phase offset between pump modulation and the sample's response (as picked up by probe) fits to sample thermal properties

	As-received	Post Solution Anneal	Heat treated 400 °C, 2.5 hrs	Heat treated 400 °C, 23 hrs
k_A ($Wm^{-1}K^{-1}$) @ 75 °C	14.3±1.2	29.3±5.9	25.2±5.0	29.6±5.9
k_M ($Wm^{-1}K^{-1}$) @ 21 °C	8.6±0.9	11.8±2.1	--	--
L (J/g)	12.8	22.8	21.7	18.2
A_f (°C)	31	31	46	58

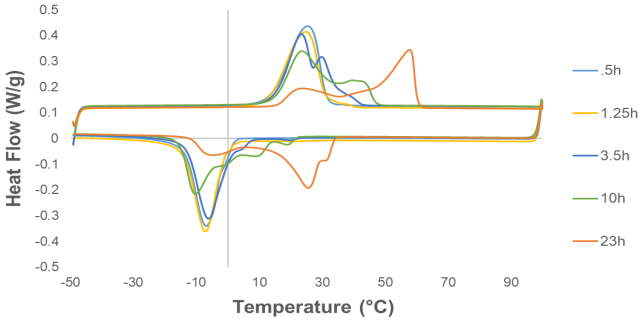

- Precipitate growth shifts transformation temperature significantly* (A_f = 31 °C → A_f= 58 °C)
- Latent heat generally decreases with increasing transformation temperature

* A_f - Austenite finish temperature

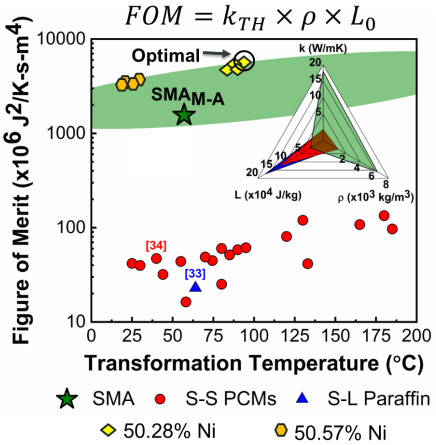

This processing makes these materials record-breaking as solid-solid PCMs

Conclusions and Future Work

- By heat-treating according to phase diagram, precipitates can be selectively grown to tailor latent heat, thermal conductivity, and transformation temperature
- Thermal conductivity switching over 2.5x observed across phase transition
- In FY20, we will:
  - explore thin-film NiTi, additively manufactured NiTi, and NiTiCu for similar material properties.
  - Explore anisotropic thermal conductivity of van der Waals materials (intercalated and unintercalated and compressed)
  - Expand efforts to includetunable thermal properties in functional and multiferroic materials

Development of Protein Catalyzed Capture Agents for the Detection of E. *coli* O157:H7 in Food

Alexander Winton[a], An Ngo[b], Matthew Coppock[a]

[a] CCDC Army Research Laboratory, Sensors and Electron Devices Directorate, Adelphi, MD 20783, United States; [a] Oak Ridge Associated Universities, Oak Ridge, TN supporting CCDC Army Research Laboratory, Adelphi, MD 20783, United States

Foodborne pathogens represent a significant health concern worldwide with the World Health Organization estimating 582 million illnesses annually with the enterohemorrhagic E. *coli* (EHEC) O157:H7 being of particular interest. Current culture based detection methods are slow and fail to detect contamination in real-time. Peptides are advantageous as they exhibit improved storage and shelf-life capabilities, are inexpensively generated by chemical synthesis, and can incorporate unnatural chemistries. This work seeks to identify E. *coli* O157:H7 specific peptide affinity ligands, developed through the protein catalyzed capture (PCC) agent method, for applications in detecting pathogen contaminated food and beverages. This research provides a foundation for future development of versatile, peptide based biosensors.

Unique E. *coli* Targets for Peptide Screening

Unique targets are identified for PCC screening based upon solvent exposure and known structure. This technique enables safe, easy screening of difficult or dangerous targets.

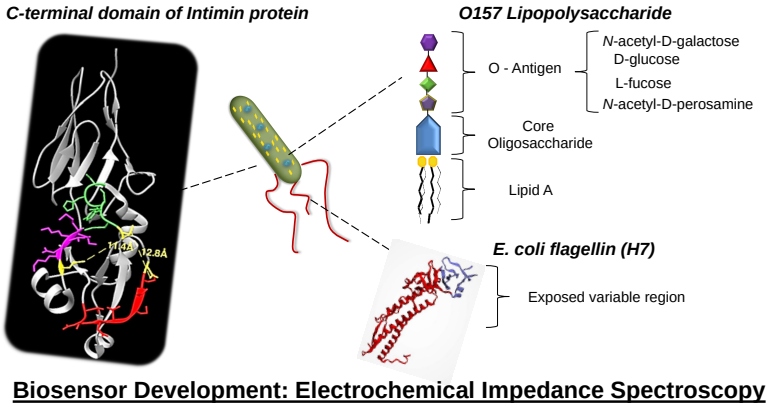

Biosensor Development: Electrochemical Impedance Spectroscopy

Gold electrodes are functionalized through thiol linkages utilizing either thiol-PEG linkers or a cysteine residue. Impedance measurements utilizing the ferricyanide/ferrocyanide redox reporter enable determination of electrode coverage by sensing ligands and subsequently, binding by a target protein.

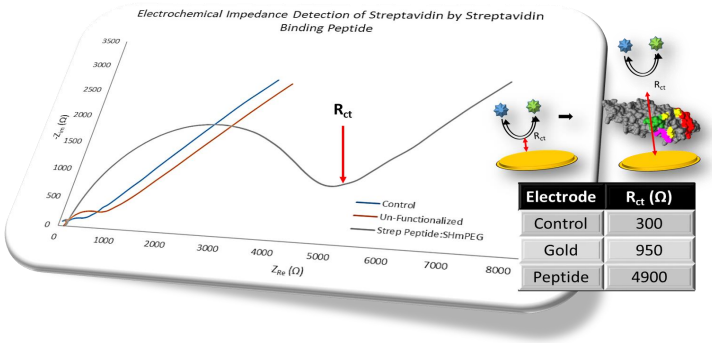

Electrode	R_{ct} (Ω)
Control	300
Gold	950
Peptide	4900

Biosensor development: Surface Plasmon Resonance

Surface Plasmon Resonance (SPR) enables determination of kinetic and thermodynamic parameters associated with target – ligand interactions. A gold surface is modified with either a protective coating, or a Streptavidin – binding peptide. Data demonstrate the ability to detect Streptavidin using peptide functionalized gold.

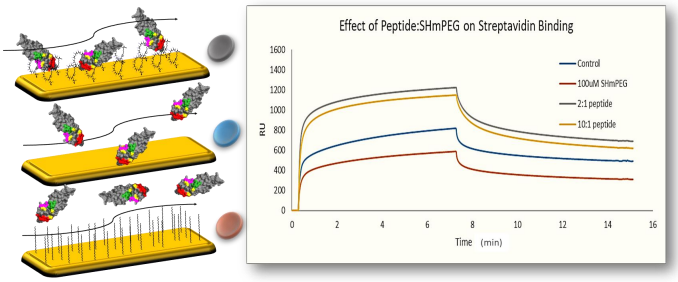

Identification of Target Binding Epitopes by OBOC Library Screening

Polystyrene beads are functionalized with D-amino acid peptides by means of standard split and mix SPPS methods. The peptides are cyclized and a click handle is then incorporated. A library of roughly 1.6 million variants is then utilized for peptide display. Initially, negative selection screening is performed to remove non-specific binders. Subsequent incubation with target SynEps enables *in situ* click interactions for determining cyclic peptide candidates. The use of an *in situ* click screen enables entropically favorable binders to be identified (common K_d of 10-100 nM obtained). Edman degradation is then performed to determine the cyclic peptide sequence.

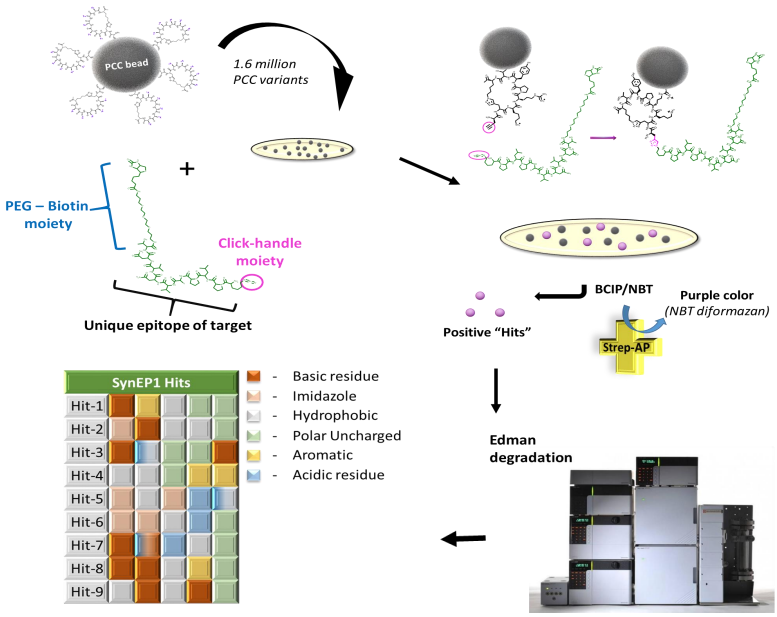

Separation of E. *coli* from Food Samples

Magnetic nanoparticles will be functionalized with cyclic peptides discovered through the OBOC library screening. The functionalized nanoparticles will bind specific E. *coli* and enable bacterial concentration by magnetic separation. This will enable improved detection times and limits for pathogens in food samples.

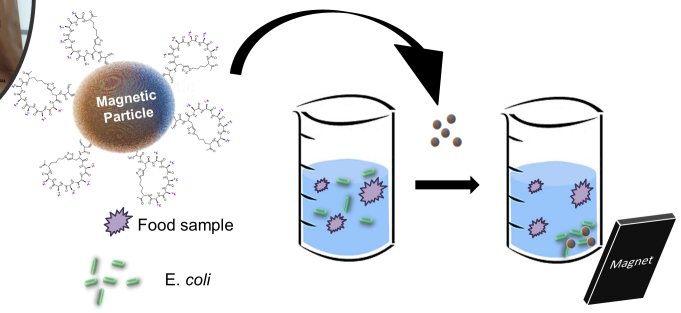

Future Directions: Wearable Biosensors

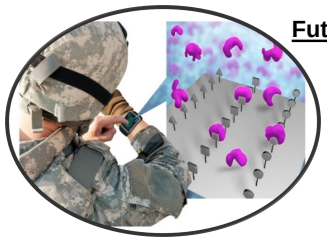

- Screen and identify PCC peptides against biomarkers relevant to human performance
- Leverage PCC peptide stability and platform adaptability for use in various sensor/assay formats
- Pursue wearable sensors capable of detecting multiple targets for integrated health/capability assessment of wearer

References

- *Kirk, M. D.; Pires, S. M.; Black, R. E.; Caipo, M.; Crump, J. A.; Devleesschauwer, B.; Dopfer, D.; Fazil, A.; Fischer-Walker, C. L.; Hald, T.; Hall, A. J.; Keddy, K. H.; Lake, R. J.; Lanata, C. F.; Torgerson, P. R.; Havelaar, A. H.; Angulo, F. J., World Health Organization Estimates of the Global and Regional Disease Burden of 22 Foodborne Bacterial, Protozoal, and Viral Diseases, 2010: A Data Synthesis. Plos Medicine 2015, 12 (12).*
- *Pettersen, E. F.; Goddard, T. D.; Huang, C. C.; Couch, G. S.; Greenblatt, D. M.; Meng, E. C.; Ferrin, T. E., UCSF chimera - A visualization system for exploratory research and analysis. Journal of Computational Chemistry 2004, 25 (13), 1605-1612.*
- *Wang, L.; Reeves, P. R., Organization of Escherichia coli O157 O antigen gene cluster and identification of its specific genes. Infection and Immunity 1998, 66 (8), 3545-3551.*
- *Das, S.; Nag, A.; Liang, J. X.; Bunck, D. N.; Umeda, A.; Farrow, B.; Coppock, M. B.; Sarkes, D. A.; Finch, A. S.; Agnew, H. D.; Pitram, S.; Lai, B.; Yu, M. B.; Museth, A. K.; Deyle, K. M.; Lepe, B.; Rodriguez-Rivera, F. P.; McCarthy, A.; Alvarez-Villalonga, B.; Chen, A.; Heath, J.; Stratis-Cullum, D. N.; Heath, J. R., A General Synthetic Approach for Designing Epitope Targeted Macrocyclic Peptide Ligands. Angewandte Chemie-International Edition 2015, 54 (45), 13219-13224.*
- *Coppock, M. B.; Stratis-Cullum, D. N., A universal method for the functionalization of dyed magnetic microspheres with peptides. Methods 2019, 158, 12-16.*

List of Symbols, Abbreviations, and Acronyms

4PECRD	4th Annual Postdoc and Early Career Research Day
ALC	Adelphi Laboratory Center
APG	Aberdeen Proving Ground
ARL	Army Research Laboratory
ARL-C	ARL Central
ARL-W	ARL West
CCDC	US Army Combat Capabilities Development Command
CISD	Computational and Information Sciences Directorate
HRED	Human Research and Engineering Directorate
PDA	postdoc association
Q&A	question and answer
SEDD	Sensors and Electron Devices Directorate
VTD	Vehicle Technology Directorate
WMRD	Weapons and Materials Research Directorate

1 (PDF)	DEFENSE TECHNICAL INFORMATION CTR DTIC OCA
3 (PDF)	CCDC ARL FCDD RLD DCI TECH LIB FCDD RLS RP A WILSON FCDD RLC IB P SHARMA